

Disclaimer: This is a pre-publication version. Readers are recommended to consult the full published version for accuracy and citation.

1 Monitoring abiotic degradation in sinking versus suspended Arctic sea ice algae  
2 during a spring ice melt using specific lipid oxidation tracers

3

4 Jean-François Rontani <sup>a\*</sup>, Simon T. Belt <sup>b</sup>, Thomas A. Brown <sup>b</sup>, Rémi Amiraux <sup>a</sup>, Michel  
5 Gosselin <sup>c</sup>, Frédéric Vaultier <sup>a</sup>, Christopher J. Mundy <sup>d</sup>

6

7

8 <sup>a</sup> Aix Marseille Université, Université de Toulon, CNRS/INSU/IRD, Mediterranean Institute of  
9 Oceanography (MIO) UM 110, 13288, Marseille, France

10

11 <sup>b</sup> Biogeochemistry Research Centre, School of Geography, Earth and Environmental  
12 Sciences, University of Plymouth, Drake Circus, Plymouth, Devon PL4 8AA, UK

13

14 <sup>c</sup> Institut des sciences de la mer (ISMER), 310 Allée des Ursulines, Université du Québec à  
15 Rimouski, Rimouski, Québec G5L 3A1, Canada

16

17 <sup>d</sup> Centre for Earth Observation Science (CEOS), Department of Environment and Geography,  
18 CHR Faculty of Environment, Earth and Resources, University of Manitoba, Winnipeg,  
19 Manitoba R3T 2N2, Canada

20

21

22

23

24 \* Corresponding author. Tel.: +33-4-86-09-06-02; fax: +33-4-91-82-96-41.

25 **ABSTRACT**

26 The abiotic degradation state of sea ice algae released during a late spring ice melt process  
27 was determined by sampling the underlying waters and measuring certain well-known algal  
28 lipids and their oxidation products, including those derived from epi-brassicasterol, 24-  
29 methylenecholesterol, palmitoleic acid and the phytol side-chain of chlorophyll. More  
30 specifically, parent lipids and some of their oxidation products were quantified in suspended  
31 (collected by filtration) and sinking (collected with sediment traps at 5 and 30 m) particles  
32 from Resolute Passage (Canada) during a period of spring ice melt in 2012 and the outcomes  
33 compared with those obtained from related sea ice samples analyzed previously. Our data  
34 show that suspended cells in the near surface waters appeared to be only very weakly affected  
35 by photooxidative processes, likely indicative of a community of unaggregated living cells  
36 with high seeding potential for further growth. In contrast, we attribute the strong  
37 photooxidation state of the organic matter in the sediment traps deployed at 5 m to the  
38 presence of senescent and somewhat aggregated sea ice algae that descended only relatively  
39 slowly within the euphotic zone, and was thus susceptible to photochemical degradation. On  
40 the other hand, the increased abiotic preservation of the sinking material collected in the  
41 sediment traps deployed at 30 m, likely reflected more highly aggregated senescent sea ice  
42 algae that settled sufficiently rapidly out of the euphotic zone to avoid significant  
43 photooxidation. This better-preserved sinking material in the deeper sediment traps may  
44 therefore contribute more strongly to the underlying sediments. A three-component  
45 conceptual scheme summarizing the abiotic behavior of Arctic sea ice algae in underlying  
46 waters is proposed.

47

48 *Keywords:* Sea ice algae; Suspended and sinking particles; Lipid oxidation products;

49 Photooxidation; Preservation; Aggregation.

50

51 **1. Introduction**

52 Sea ice is a key parameter in controlling global climate (Ferrari et al., 2014) and within  
53 the polar regions, in particular, due to its influence on surface albedo (Hartmann, 1994; Curry  
54 et al., 1995) and by providing a physical barrier that limits the exchange of heat, moisture and  
55 gases between the ocean and the atmosphere. The extent, nature and seasonality of sea ice  
56 also impacts on polar marine ecosystems across all trophic levels, not least at the base of the  
57 food web, where it provides a physical environment suitable for the development and growth  
58 of ice algal communities and a range of heterotrophic eukaryotes (Róžańska et al., 2009;  
59 Caron and Gast, 2010). The bottom (ca. 10 cm) sections of annually formed Arctic sea ice  
60 comprises an interstitial community of ice crystals, brine pockets and a network of channels  
61 and capillaries that provide a host for the growth of an adapted community of microalgae  
62 (Horner et al., 1992; Arrigo et al., 2010) that represent a critical food source for ice-associated  
63 and pelagic herbivorous protists (Michel et al., 2002) and metazoans (Nozais et al., 2001).  
64 Such is the importance of this community, it has been estimated that the contribution of sea  
65 ice algae to total primary production is ca. 3–25% on Arctic shelves (e.g., Legendre et al.,  
66 1992) and as much as 57% in the central Arctic Ocean (Gosselin et al., 1997). During the  
67 early stages of ice melt, and prior to ice break-up, ice algae are released from bottom ice into  
68 the water column, where they can make a significant contribution to the cycling of organic  
69 carbon throughout the Arctic (e.g., Michel et al., 2006). In addition to the production of  
70 photosynthetic pigments (e.g., chlorophyll) and storage lipids (e.g., fatty acids) common to all  
71 microalgae, sea ice algae also produce extracellular polymeric substances (EPS), which play  
72 multiple roles in the entrapment, retention and survival of these organisms within the sea ice  
73 matrix (Ewert and Deming, 2013). Further, the production of EPS not only facilitates the  
74 attachment of algae to the ice substrate itself, but also the formation of microaggregates of

75 algal cells that can remain intact after ice melt (Riebesell et al., 1991). As a result, the  
76 sedimentation of ice algae can be enhanced relative to otherwise isolated cells that tend to  
77 remain in suspension or, at least, have longer residence times in near surface waters.

78 Elucidation of the fate of algal material in the water column during and after sea ice  
79 melt in the Arctic constitutes a very important challenge (Tedesco et al., 2012; Vancoppenolle  
80 et al., 2013). It is generally considered that a part (until now not estimated) of this strong  
81 pulse of particulate organic matter (POM), which is not degraded by bacteria or grazed by  
82 heterotrophs such as zooplankton during its descent to the seafloor, may be stored in  
83 sediments (Fortier et al., 2002; Renaud et al., 2007). However, the integrity of the OM in such  
84 settings remains largely unexamined.

85 Although less widely studied than its biologically mediated (heterotrophic)  
86 counterpart, photooxidative degradation is now known to play a significant role in the fate of  
87 POM in the open ocean (Rontani, 2008; Estapa and Mayer, 2010), with photosensitization  
88 playing an important role in the photodegradation of algal detritus (Nelson, 1993; Mayer et  
89 al., 2009). Due to the presence of chlorophyll and pheopigments, which are well-known  
90 sensitizers of Type II photooxidation processes (i.e. involving singlet oxygen ( $^1\text{O}_2$ ); Kessel  
91 and Smith, 1989), and the longer lifetime of  $^1\text{O}_2$  in lipid-rich membranes compared to aqueous  
92 solution (Suwa et al., 1977), Type II photosensitized oxidation processes act intensively in  
93 senescent algae (Rontani, 2012). Such processes afford hydroperoxides, which, after  
94 subsequent homolytic cleavage, are responsible for the induction of autoxidation (free radical-  
95 induced oxidation) processes (Girotti, 1998; Rontani et al., 2003). It has also been  
96 demonstrated that Type II photosensitized oxidation appears to be particularly efficient in  
97 natural samples in the Arctic (Rontani et al., 2012) and also in senescent phytoplanktonic cells  
98 under in vitro conditions, despite low temperatures and irradiances (Amiriaux et al., 2016).  
99 This apparent paradox has been attributed to a combination of the relative preservation of the

100 sensitizer (chlorophyll) at low irradiances, which permits a longer production time for  $^1\text{O}_2$ ,  
101 and the slower diffusion rate of  $^1\text{O}_2$  through the cell membranes at low temperatures  
102 (Ehrenberg et al., 1998), thus favoring the intra-cellular involvement of Type II  
103 photosensitized reactions. Potentially, therefore, the low irradiance and low temperature  
104 conditions that are characteristic of the under-ice environment in the Arctic could strongly  
105 favor the photodegradation of algae released by melting sea ice. However, it is also important  
106 to note that these photodegradation processes are also strongly dependent on both the  
107 residence time of cells within the euphotic layer (Zafiriou et al., 1984; Mayer et al., 2009) and  
108 the physiological state of the phytoplanktonic cells themselves (Merzlyak and Hendry, 1994;  
109 Nelson, 1993). Indeed,  $^1\text{O}_2$  production can exceed the quenching capacities of the  
110 photoprotective system (and thus induce cell damage) only when the photosynthetic pathways  
111 are not operative, as is the case for senescent or highly stressed cells (Nelson, 1993).  
112 Interestingly, Ligowski et al. (1992) previously failed to detect photosynthesis in diatoms  
113 from brash ice after ice melting, while Ralph et al. (2007) concluded that sea ice algal cells  
114 are more susceptible to photosynthetic stress during ice melt compared to their incorporation  
115 into the ice matrix during the freezing process. The involvement of photochemical damage in  
116 sea ice algal material released during ice melt is thus very likely. However, by recording rates  
117 of oxygen production and consumption between aggregated and dispersed ice algae, Riebesell  
118 et al. (1991) suggested that metabolically less active ice algae tend to be concentrated in  
119 aggregates, while growing cells are more likely to remain unaggregated. As a result, the  
120 organic content of suspended and sinking sea ice material might be expected to exhibit  
121 contrasting photo-oxidation states.

122         The purpose of this study, therefore, was to apply a suite of specific lipid oxidation  
123 tracers (Fig. 1) to monitor the degradation of sea ice algae in suspended (collected by  
124 filtration) and sinking (collected with sediment traps) particles from Resolute Passage

125 (Canada) during a period of spring ice melt (but continuous sea ice cover), and for which the  
126 corresponding sea ice algal lipid composition and degradation state had previously been  
127 established (Rontani et al., 2014). In particular, we aimed to compare the degradation states of  
128 suspended and sinking OM during the early stages of ice melt, and to identify how the  
129 sensitivity of the released sea ice algal-derived OM towards photodegradation was dependent  
130 on the aggregation state of the algal cells.

131 With the specific aim of characterizing the abiotic (photo-oxidation) degradation state  
132 of sea ice algal material in the water column, we focused our analyses on chlorophyll and a  
133 range of lipids along with some of their degradation products (Fig. 1). Such lipids included  
134 certain diatom-derived highly branched isoprenoid (HBI) alkenes (including IP<sub>25</sub>, which is  
135 made uniquely by sea ice diatoms, Belt et al., 2007; 2013; Brown et al., 2014), the mono-  
136 unsaturated fatty acid C<sub>16:1 $\omega$ 7</sub> (palmitoleic acid; the dominant monounsaturated fatty acid of  
137 sea-ice algae, Fahl and Kattner, 1993; Leu et al., 2010), together with the  $\Delta^5$ -sterols 24-  
138 methylcholesta-5,22*E*-dien-3 $\beta$ -ol (termed epi-brassicasterol here since diatoms synthesize the  
139 24 $\alpha$ -isomer) and 24-methylcholesta-5,24(28)-dien-3 $\beta$ -ol (24-methylenecholesterol) (generally  
140 considered to be specific to phytoplankton, Volkman, 1986; 2003). The analysis of other  
141 common lipids such as C<sub>18:1 $\omega$ 9</sub> (oleic acid), cholest-5-en-3 $\beta$ -ol (cholesterol), 24-  
142 methylcholest-5-en-3 $\beta$ -ol (campesterol) and 24-ethylcholest-5-en-3 $\beta$ -ol (sitosterol) was not  
143 included in this study as they are not sufficiently specific to sea ice algal or phytoplankton  
144 sources.

145

## 146 **2. Experimental**

### 147 *2.1. Study location and sample collection*

148 This study was conducted in 2012 at a landfast ice station (74° 43.613' N, 95° 33.496'  
149 W; water column depth: 90 m) located between Griffith Island and Sheringham Point

150 (Cornwallis Island) in Resolute Passage, Nunavut, Canada. The thickness of the first-year ice  
151 was ca. 1.27 m at the beginning of the sampling period (Galindo et al., 2015). From 22 May to  
152 20 June 2012, suspended particulate matter (SPM) samples were collected at 2, 5 and 10 m  
153 with 5 l Niskin bottles. From 18 May to 23 June, sediment trap samples were collected with  
154 two Hydro-Bios multi-sediment traps MS12 that were deployed at 5 m and 30 m from the  
155 undersurface of the ice. The interceptor traps, fixed to a tripod on the sea ice, were made of  
156 polyvinyl chloride (PVC) with an internal diameter of 13 cm and an aspect ratio  
157 (height:diameter) of 4. Each trap was fitted with a plastic baffle mounted in the opening, to  
158 prevent the entrance of larger organisms. In the receiving cups, a 5% buffered formalin-  
159 seawater solution was used as a preservative (Hargrave et al., 2002). The trap rotation interval  
160 was every three days. Upon recovery, samples were stored at 4 °C in the dark until further  
161 analysis. Sub-samples for lipid analysis were filtered onto Whatman GF/F 47 mm filters, kept  
162 frozen at -80 °C, then lyophilized before sending them to the Plymouth laboratory.

163 Photochemically Active Radiation (PAR) at 5 and 30 m underneath the ice was estimated  
164 from vertical profiles made with a scalar PAR sensor (Biospherical QSP-2300) mounted on a  
165 Sea-Bird SBE 19plus V2 conductivity-temperature-depth (CTD) probe.

166 Although the presence of formalin would have prevented biotic degradation, the same  
167 may not have been entirely the case for abiotic degradation processes in the sediment traps,  
168 with some autoxidation possibly having taking place, even in the absence of light. In contrast,  
169 the shading effect of the trap material on the receiving flasks and the thickness of their plastic  
170 layer, likely minimized or even prevented photodegradation processes entirely, such that these  
171 are considered to have been negligible. Overall, the intensity of autoxidation and  
172 photooxidation processes, which did not increase significantly with sampling time, suggest  
173 that abiotic processes were not significant during the time series.

174

175 2.2. *Sample treatment*

176 Contents of HBIs and oxidation products of other lipids ( $\Delta^5$ -sterols, fatty acids and  
177 chlorophyll phytyl side-chain) were determined separately on individual samples (filters). The  
178 treatment of filters for HBI analysis (alkaline hydrolysis and purification by open column  
179 chromatography) and lipid oxidation product measurement ( $\text{NaBH}_4$  reduction and alkaline  
180 hydrolysis) was performed as described previously (Brown et al., 2011; Rontani et al., 2014).

181

182 2.3. *Derivatization*

183 For extracts containing hydroxyl functions (i.e. sterols, fatty acids and oxidation  
184 products), samples were derivatized by dissolving them in 300  $\mu\text{l}$  of a mixture of pyridine and  
185 BSTFA (Supelco; 2:1, v/v) and silylated (1 h) at 50  $^\circ\text{C}$ . After evaporation to dryness under a  
186 stream of  $\text{N}_2$ , the derivatized residue was dissolved in a mixture of hexane and BSTFA (to  
187 avoid desilylation) and analyzed by GC-MS-MS or GC-QTOF.

188

189 2.4. *Gas chromatography/electron impact mass spectrometry (GC-EIMS)*

190 HBIs were analyzed and quantified by GC-EIMS in Selective Ion Monitoring (SIM)  
191 mode ( $m/z$  350.3, 348.3, 346.3, limit of detection = 1 ng/l) using an Agilent 7890A gas  
192 chromatograph coupled to an Agilent 5975c quadrupole mass spectrometer (GC-MS; HP5ms;  
193 Belt et al., 2012). Comparison of retention indices and mass spectra of HBIs in sample  
194 extracts to those obtained from purified standards permitted unambiguous identification.

195 Quantification of HBIs was achieved by comparison of SIM peak areas with those of the  
196 internal standard (9-octylheptadec-8-ene; 2 ng) and normalised to individual response factors  
197 (Belt et al., 2012) and sample volumes.

198

199 2.5. *Gas chromatography-electron ionization tandem mass spectrometry (GC-MS-MS)*



200 Fatty acids, phytol and their oxidation products were identified and quantified using an  
201 Agilent 7890A/7000A tandem quadrupole gas chromatograph system (Agilent Technologies,  
202 Parc Technopolis - ZA Courtaboeuf, Les Ulis, France). A cross-linked 5% phenyl-  
203 methylpolysiloxane (Agilent; HP-5MS) (30 m × 0.25 mm, 0.25 μm film thickness) capillary  
204 column was employed. Analyses were performed with a multi-mode injector operating in  
205 splitless mode (with 0.5 min splitless period) set at 270 °C and the oven temperature  
206 programmed from 70 °C to 130 °C at 20°C/min, then to 250 °C at 5 °C/min and then to 300  
207 °C at 3 °C/min. The pressure of the carrier gas (He) was maintained at  $0.69 \times 10^5$  Pa until the  
208 end of the temperature program and then programmed from  $0.69 \times 10^5$  Pa to  $1.49 \times 10^5$  Pa at  
209  $0.04 \times 10^5$  Pa/min. The following mass spectrometric conditions were employed: electron  
210 energy, 70 eV; source temperature, 230 °C; quadrupole 1 temperature, 150 °C; quadrupole 2  
211 temperature, 150 °C; collision gas (N<sub>2</sub>) flow, 1.5 ml/min; quench gas (He) flow, 2.25 ml/min;  
212 mass range, 50–700 Da; cycle time, 313 ms. Quantification of analytes was carried out with  
213 external standards in Multiple Reaction Monitoring (MRM) mode. MRM transitions were  
214 selected after CID (Collision Induced Dissociation) analyses of all the precursor ions  
215 corresponding to the more intense fragment ions observed in EI mass spectra of the  
216 compounds of interest.

217

218 *2.6. Gas chromatography–electron ionization quadrupole time of flight mass spectrometry*  
219 *(GC–QTOF)*

220  $\Delta^5$ -sterols and their oxidation products were identified and quantified with an Agilent  
221 7890B/7200 GC–QTOF System (Agilent Technologies, Parc Technopolis - ZA Courtaboeuf,  
222 Les Ulis, France). A cross-linked 5% phenyl-methylpolysiloxane (Agilent; HP-5MS ultra  
223 inert) (30 m × 0.25 mm, 0.25 μm film thickness) capillary column was employed. Analyses  
224 were performed with an injector operating in pulsed splitless set at 280 °C and the oven

225 temperature programmed from 70 °C to 130 °C at 20 °C/min, then to 250 °C at 5 °C/min and  
226 then to 300 °C at 3 °C/min. The pressure of the carrier gas (He) was maintained at  
227  $0.69 \times 10^5$  Pa until the end of the temperature program. Instrument temperatures were 300 °C  
228 for transfer line and 230 °C for the ion source. Accurate mass spectra were recorded across  
229 the range  $m/z$  50–700 at 4 GHz. The QTOF MS instrument provided a typical resolution  
230 ranging from 8009 to 12252 from  $m/z$  68.9955 to 501.9706. Perfluorotributylamine (PFTBA)  
231 was utilized for daily MS calibration. Identification and quantification were carried out with  
232 external standards in Time of Flight (TOF) mode.

233

### 234 2.7. Chlorophyll analyses

235 Duplicate sub-samples were filtered through 25 mm Whatman GF/F filters.  
236 Chlorophyll *a* retained on the filters was measured using a 10-005R Turner Designs  
237 fluorometer, after extraction in 90% acetone for 18 h at 4 °C in the dark (acidification method  
238 of Parsons et al. (1984)). The fluorometer was calibrated with a commercially available  
239 chlorophyll *a* standard (from *Anacystis nidulans*, Sigma).

240

### 241 2.8. Lipid oxidation products employed as tracers

#### 242 2.8.1. Chlorophyll *a*

243 Although it has been shown that the visible light-dependent degradation rate of the  
244 tetrapyrrole ring in chlorophyll *a* (chl *a*) is three to five times higher than that of the phytol  
245 side-chain (Cuny et al., 1999; Christodoulou et al., 2010), no specific and stable  
246 photodegradation products of the former have been identified in the literature. In contrast,  
247 Type II photosensitized oxidation (i.e. involving  $^1O_2$ ) of the phytol side-chain leads to the  
248 well-known production of 2-hydroperoxy-3-methylidene-7,11,15-trimethylhexadecan-1-ol  
249 which, after  $NaBH_4$  reduction, can be quantified as 3-methylidene-7,11,15-

250 trimethylhexadecan-1,2-diol (phytyldiol) (Rontani et al., 1994) (Fig. 1). Indeed, phytyldiol is  
251 ubiquitous in the marine environment and constitutes a stable and specific tracer for the  
252 photodegradation of the chlorophyll phytyl side-chain (Rontani et al., 1996; Cuny and  
253 Rontani, 1999). Further, the molar ratio phytyldiol:phytol (Chlorophyll Phytyl side-chain  
254 Photodegradation Index, CPPI) has been proposed to estimate the extent of photodegradation  
255 of chlorophylls possessing a phytyl side-chain in natural marine samples through use of the  
256 empirical equation: chlorophyll photodegradation % =  $(1 - [\text{CPPI} + 1]^{-18.5}) \times 100$  (Cuny et al.,  
257 1999). The chlorophyll phytyl side-chain is also sensitive to free radical oxidation  
258 (autoxidation) reactions. *Z*- and *E*- 3,7,11,15-tetramethylhexadec-3-ene-1,2-diols and  
259 3,7,11,15-tetramethylhexadec-2-ene-1,4-diols have been proposed previously as tracers of  
260 these processes (Rontani and Aubert, 2005) (Fig. 1).

261

### 262 2.8.2. HBI alkenes

263 The biomarker 2,6,10,14-tetramethyl-7-(3-methylpent-4-enyl)-pentadecane (IP<sub>25</sub>; 'Ice  
264 Proxy with 25 carbon atoms'; Belt et al., 2007) is produced by certain Arctic sea ice diatoms  
265 during the spring sea ice algal bloom (March–May) (Brown et al., 2011; 2014; Belt et al.,  
266 2013) and has been used in a number of studies to provide proxy-based evidence for palaeo  
267 sea ice occurrence for several Arctic regions (Belt and Müller, 2013) and as a tracer for the  
268 incorporation of sea ice algal OM into Arctic food webs (Brown and Belt, 2012a; 2012b). Sea  
269 ice diatoms also produce smaller quantities of HBI trienes with tri-substituted double bonds  
270 such as 2,6,10,14-tetramethyl-7-(3-methylpenta-1,4-dienyl)-pentadeca-7(2*E*),9*E/Z*-dienes  
271 (Belt et al., 2007; Brown, 2011). Due to the presence of two tri-substituted double bonds that  
272 are very reactive towards <sup>1</sup>O<sub>2</sub> and a *bis*-allylic carbon atom (where hydrogen abstraction is  
273 highly favored), these specific HBI trienes are particularly sensitive to photooxidation  
274 (Rontani et al., 2011) and autoxidation (Rontani et al., 2014). However, it is not possible to

275 quantify their photoproducts due to further (and rapid) oxidation of the primary products  
276 (Rontani et al., 2014). In contrast, the mono-unsaturated HBI IP<sub>25</sub>, only possesses a single low  
277 reactivity methyldiene group, and is thus essentially unaffected by these two abiotic  
278 degradation processes. As a consequence, the ratio between these two HBI lipids  
279 (C<sub>25:3</sub>(E)/IP<sub>25</sub>) constitutes a potentially very useful tool for estimating changes to the  
280 degradation state of sea ice algae.

281

### 282 2.8.3. Monounsaturated fatty acids

283 Autoxidation and photooxidation of monounsaturated fatty acids lead to the formation  
284 of oxidation products that are sufficiently stable in the marine environment to act as tracers of  
285 abiotic degradation processes (Rontani, 2012). <sup>1</sup>O<sub>2</sub>-mediated photooxidation of palmitoleic  
286 acid, for example, produces a mixture of 9- and 10-hydroperoxides with an allylic *trans*-  
287 double bond (Frankel et al., 1979), which can subsequently undergo highly stereoselective  
288 radical allylic rearrangement to 11-*trans* and 8-*trans* hydroperoxides, respectively (Porter et  
289 al., 1995) (Fig. 1). In contrast, autoxidation (free radical-induced oxidation) affords a mixture  
290 of 9-*trans*, 10-*trans*, 11-*trans*, 11-*cis*, 8-*trans*, and 8-*cis* hydroperoxides (Frankel, 1998) (Fig.  
291 1). For the current study, therefore, the relative importance of autoxidative and photooxidative  
292 degradation of palmitoleic acid was estimated on the basis of the proportion of its specific *cis*-  
293 oxidation products and of the water temperature according to the approach described  
294 previously by Marchand and Rontani (2001).

295

### 296 2.8.4. $\Delta^5$ -sterols

297 <sup>1</sup>O<sub>2</sub>-mediated photooxidation of  $\Delta^5$ -sterols produces mainly  $\Delta^6$ -5 $\alpha$ -hydroperoxides  
298 with smaller amounts of  $\Delta^4$ -6 $\alpha$ /6 $\beta$ -hydroperoxides (Kulig and Smith, 1973), while their  
299 autoxidation yields mainly 7 $\alpha$ - and 7 $\beta$ -hydroperoxides and, to a lesser extent, 5 $\alpha$ / $\beta$ , 6 $\alpha$ / $\beta$ -

300 epoxysterols and  $3\beta,5\alpha,6\beta$ -trihydroxysterols (Smith, 1981). On the basis of their stabilities  
301 and specificities,  $\Delta^4$ -stera- $3\beta,6\alpha/\beta$ -diols (resulting from  $\text{NaBH}_4$ -reduction of  $\Delta^4$ - $6\alpha/6\beta$ -  
302 hydroperoxides) and  $3\beta,5\alpha,6\beta$ -steratriols were previously selected as tracers of  $\Delta^5$ -sterol  
303 photooxidation and autoxidation, respectively (Rontani et al., 2009) (Fig. 1), and the extent of  
304 these degradation processes may be estimated using different equations previously proposed  
305 by Christodoulou et al. (2009). It may also be noted that, in the case of di-unsaturated sterols,  
306 autoxidation estimates are not possible due to the additional attack of the double bond of the  
307 lateral chain precluding  $3\beta,5\alpha,6\beta$ -steratriol accumulation.

308

#### 309 2.8.5. Production of standard oxidation products

310 Standard oxidation products of monounsaturated fatty acids, chlorophyll phytol side-  
311 chain, and  $\Delta^5$ -sterols were obtained according to previously described procedures (Rontani  
312 and Marchand, 2000; Marchand and Rontani, 2001; Rontani and Aubert, 2005).

313

### 314 3. Results

#### 315 3.1. SPM samples

316 The concentration of chl *a* was measured in all the SPM samples and showed a clear  
317 increase at 2 m from 30 May to 11 June (Table 1). On the other hand, quantification of phytol  
318 and phytyldiol allowed us to show that the photooxidation percentage of chlorophyll in the  
319 different SPM samples was relatively low, particularly at 2 m, with values ranging from 0–  
320 30% (Fig. 2A). At 5 m and 10 m, the photooxidation percentage reached 50% and 40%,  
321 respectively (Fig. 2B and C). In contrast, we failed to detect autoxidation products of  
322 chlorophyll phytol side-chain in any of the SPM samples.

323 The  $C_{25:3}(E)/IP_{25}$  ratios (g/g) in the SPM from 22 May to 03 June ( $0.219 \pm 0.062$ ,  
324  $0.313 \pm 0.096$  and  $0.246 \pm 0.059$  at 2, 5 and 10 m, respectively) (Table 2) were close to that  
325 measured in the corresponding bottom (0–3 cm) sea ice ( $0.244 \pm 0.235$  g/g) (Belt et al., 2013).

326 Within the fatty acids, the SPM was dominated by palmitoleic acid, as expected, with a  
327 strong increase in the concentration of all components at 2 m from 30 May to 07 June (Fig.  
328 3A). A general decrease in the concentration of fatty acids could be observed with depth,  
329 however (Fig. 3B and C). Quantification of the photo- and autoxidation products of  
330 palmitoleic acid confirmed the very weak abiotic degradation state of the material collected at  
331 2 m between 30 May and 7 June (Fig. 4A). Similar trends could also be observed at 5 and 10  
332 m (Fig. 4B and C). Finally, consistent with the profiles of chl *a* and palmitoleic acid, the  
333 concentrations of epi-brassicasterol and 24-methylenecholesterol at 2 m increased  
334 significantly from 30 May to 07 June (Table 1). However, no photooxidation products of epi-  
335 brassicasterol and 24-methylenecholesterol could be detected in any of the SPM samples.

336

### 337 3.2. Sediment trap samples

338 The fluxes of chl *a* appeared to be very distinct at the two depths investigated (5 and 30  
339 m). Indeed, the flux of chl *a* remained relatively low ( $< 0.06$  mg/m<sup>2</sup>/d) at 5 m prior to a rapid  
340 increase to  $0.58$  mg/m<sup>2</sup>/d from 17 June to 23 June (Fig. 5A). In contrast, generally higher  
341 fluxes of chl *a* were identified at 30 m, with values ranging from 0.1–0.45 mg/m<sup>2</sup>/d (Fig. 5C).  
342 CPPI-based chlorophyll photooxidation estimates ranged from 40–100% at 5 m during the  
343 first part of the time series, before a rapid decrease occurred from 11 June to 23 June (Fig.  
344 5B). In contrast, chlorophyll was only relatively weakly photooxidized at 30 m throughout the  
345 sampling period (CPPI values ranging from 5 to 35%) (Fig. 5D). Autoxidation of the  
346 chlorophyll phytol side-chain appeared to be very weak in all of the samples of sinking  
347 particles investigated.

348 The mean values of the  $C_{25:3}(E)/IP_{25}$  ratio (g/g) in the sediment traps ( $0.004 \pm 0.008$  and  
349  $0.142 \pm 0.051$  at 5 and 30 m, respectively) (Table 3) were lower than those for the  
350 corresponding sea ice ( $0.244 \pm 0.235$ ) (Belt et al., 2013) and SPM samples (any depth, see  
351 earlier values) indicating a high degree of abiotic degradation of material collected at 5 m, yet  
352 relative preservation at 30 m. The fluxes of (total) fatty acids (Fig. 6A and B) paralleled those  
353 of chl *a* (Fig. 5A and C) at both depths, with substantially increased values towards the end of  
354 sampling at 5 m and higher (and more consistent) values at 30 m. In addition, the fatty acid  
355 profiles at 30 m exhibited a strong dominance of  $C_{16:0}$  (palmitic) and palmitoleic acids (Fig.  
356 6B) as observed previously in the corresponding sea ice samples (Rontani et al., 2014). The  
357 identification of 8-*trans*, 9-*trans*, 10-*trans* and 11-*trans* allylic hydroxyhexadecenoic acids as  
358 the major palmitoleic acid oxidation products indicated that the degradation mainly resulted  
359 from the involvement of photooxidative processes, while quantification of the products of  
360 palmitoleic acid showed that the extent of oxidation was lower at 30 m (Fig. 7B) compared to  
361 5 m (Fig. 7A).

362 Similar degradation trends could also be observed for the two diatom sterols epi-  
363 brassicasterol and 24-methylenecholesterol. Thus, only small proportions of oxidation  
364 products of epi-brassicasterol and 24-methylenecholesterol were found at 30 m (Fig. 8B and  
365 D), while quantification of the same sterols and of their oxidation products at 5 m gave  
366 evidence for strongly photodegraded algal material from 02 June to 14 June (Fig. 8A and C).  
367 Interestingly, the extent of photo-oxidation of 24-methylenecholesterol was greater than that  
368 of epi-brassicasterol, consistent with previous observations made in sea ice (Rontani et al.,  
369 2014) and in suspended particles collected in the Beaufort Sea (Rontani et al., 2012). The  
370 presence of an under-ice bloom at the end of the time series could also be observed at both  
371 depths (Fig. 8).

372

373 **4. Discussion**

374 During the period investigated, sea ice thickness reduced from 127 to 93 cm and snow  
375 cover from 16 to 4 cm. As a result of decreased snow cover, the under-ice PAR increased  
376 from 5 to 200  $\mu\text{mol photons/m}^2/\text{s}$  and from 0.5 to 32  $\mu\text{mol photons/m}^2/\text{s}$  at 5 and 30 m depth,  
377 respectively. Under-ice seawater exhibited relatively consistent hydrographic conditions with  
378 temperature ranging from  $-1.4$  to  $-1.8$   $^{\circ}\text{C}$  and salinity from 31.5 to 32.4 between 2 and 80 m  
379 (Brown et al., 2016).

380

381 *4.1. SPM samples*

382 The highest concentrations of palmitoleic acid and the two sterols, epi-brassicasterol  
383 and 24-methylenecholesterol, observed in the near surface waters (2 m) during the early  
384 sampling dates (Fig. 3A, Table 1), is consistent with quantitative estimates of sea ice algae  
385 released during the first phase of ice melt representing close to 100% of the total particulate  
386 organic carbon (POC) (Brown et al., 2016).

387 A small (ca. 4 day) lag, however, was observed for peak chl *a* compared to the lipid  
388 tracers (Table 1) which we attribute to the likely additional release of cyanobacteria,  
389 especially since these autotrophic organisms contain lower proportions of palmitoleic acid  
390 compared to diatoms, do not synthesize sterols (Volkman, 2003; 2005) and may comprise up  
391 to 7% of the microbial community of Arctic sea ice (Bowman et al., 2012).

392 With respect to degradation, the efficiency of type II photo-processes upon HBI  
393 alkenes and other well-known phytoplanktonic lipids was previously determined in senescent  
394 cells of the diatom *Haslea ostrearia* (Rontani et al., 2011) and the following order of  
395 reactivity was demonstrated:  $\text{C}_{25:3}\text{HBI} > \text{palmitoleic acid or chlorophyll phytyl side-chain} >$   
396  $\Delta^5\text{-sterols}$ ). Although a similar trend in photodegradation might, therefore, have been  
397 observed in the SPM samples, in practice, this degradation pathway appeared to have had



398 little or no effect on these lipids. For example, no photodegradation products of epi-  
399 brassicasterol and 24-methylenecholesterol could be identified in any of the SPM samples  
400 investigated, while only relatively small amounts of photooxidation products of palmitoleic  
401 acid could be detected in samples collected after 11 June 2012 (Fig. 4). Photooxidation of  
402 chlorophyll (based on CPPI calculations) (Cuny et al., 1999) was also relatively weak at 2 m,  
403 although it increased slightly with depth (Fig. 2), and the inefficiency of photodegradation  
404 processes on the SPM was particularly evident through the observation of relatively high  
405 values of the  $C_{25:3}(E)/IP_{25}$  ratio (Table 2). Interestingly, the very weak photodegradation state  
406 of palmitoleic acid and chlorophyll in the 2 m SPM samples from 30 May to 07 June  
407 coincides with the period of maximum release of algal material from the melting ice (Brown  
408 et al., 2016). Overall, our data suggest that, despite the low water temperature and irradiance  
409 under the ice, which could potentially have enhanced Type II photosensitized oxidation of  
410 algal components (Amiriaux et al., 2016), the algal cells released by sea ice and which  
411 remained suspended in the near surface waters, were in a healthy state, and that these  
412 relatively unaggregated particles were largely unaffected by photooxidative damage. Indeed,  
413 in healthy cells, the greater part of the photo-excited chlorophyll singlet state is used in the  
414 fast photochemical reactions of photosynthesis. The very small amount of the longer live  
415 triplet state resulting from intercrossing system (ICS) (Knox and Dodge, 1985), which can  
416 generate  $^1O_2$  by reaction with ground state oxygen ( $^3O_2$ ) via Type II processes, is efficiently  
417 quenched by the photo-protective system of the cells (Foote, 1976). Such data and  
418 interpretations support the hypothesis of Riebesell et al. (1991), that growing cells released by  
419 sea ice remain unaggregated (i.e. mainly in suspension), thereby increasing their seeding  
420 potential. Interestingly, the release of ice algae in good healthy state in the course of melting  
421 provides a continuous food source for under-ice grazers.

422 Quantification of the oxidation products of palmitoleic acid also enabled us to estimate  
423 the role of autoxidation processes in the degradation of suspended algal material. Although  
424 some samples of SPM exhibited relatively high autoxidation percentages (values reaching  
425 65%) (Fig. 4), those collected at 2 m between 30 May and 07 June (Fig. 4A) were only  
426 weakly affected by these processes, consistent with the SPM comprising nearly all (ca. 100%;  
427 Brown et al., 2016) of the recently deposited ice-derived POC at this time.

428

#### 429 4.2. Sediment trap samples

430 At 5 m, the fluxes of IP<sub>25</sub> (Table 3), epi-brassicasterol (Fig. 8A) and 24-  
431 methylenecholesterol (Fig. 8C) increased significantly on 02 June and remained relatively  
432 high until 05 June, suggesting the occurrence of intensified settling of aggregated sea ice algal  
433 material to the traps during this period. Interestingly, quantitative estimates of the percentage  
434 of ice-derived POC (within total POC) also increased considerably from 11–60% between 30  
435 May and 03 June (Brown et al., 2016). Although increases of the fatty acid concentration (Fig.  
436 6A) and chl *a* content (Fig. 5A) were also evident, this deposition event was less noticeable  
437 for these lipids compared to IP<sub>25</sub> and the sterols, probably due to their well-known lower  
438 biotic (Atlas and Bartha, 1992) and abiotic (Rontani et al., 1998; Christodoulou et al., 2010)  
439 stability. The strong contribution of sea ice algae to the sediment trap material is further  
440 evidenced by the similarity in the values of the (phytol + oxidation products)/IP<sub>25</sub> ratio  
441 (ranging from 300–635 g/g) with those determined previously for the bottom (0–3 cm)  
442 sections of the corresponding sea ice cores (ranging from 45–750 g/g) (Rontani et al., 2014).  
443 However, in contrast to the SPM samples, very high proportions of oxidation products of epi-  
444 brassicasterol and 24-methylenecholesterol were also detected in the 5 m sediment trap  
445 samples (Fig. 8A and C) indicating that the sea ice algae in these sinking particles had  
446 undergone a strong degree of photooxidation state prior to deposition. In addition, the extent

447 of photodegradation was greater for 24-methylenecholesterol (mainly derived from diatoms,  
448 Volkman, 1986, 2003; Rampen et al., 2010) compared to epi-brassicasterol (arising from  
449 diatoms and/or prymnesiophytes, Volkman 1986, 2003), consistent with similar observations  
450 in the corresponding sea ice samples (Rontani et al., 2014) and in particles from the Beaufort  
451 Sea (Rontani et al., 2012). This difference in photoreactivity between the two sterols was  
452 previously attributed to a higher content of mycosporine-like amino acids that are known to  
453 protect cells from reactive oxygen species such as  $^1\text{O}_2$  (Suh et al., 2003) in prymnesiophytes  
454 (Elliott et al., 2015). The very strong oxidation state of deposited sea ice algal material was  
455 further evidenced by the very low values of the  $\text{C}_{25:3}(E)/\text{IP}_{25}$  ratio (Table 3), the strong  
456 photooxidation state of chlorophyll (Fig. 5B) and relatively high proportions of the oxidation  
457 products of palmitoleic acid (Fig. 7A). Identification and quantification of the latter also  
458 enabled us to demonstrate that the degradation of these sinking particles mainly involved  
459 photooxidation, with only a minor contribution from autoxidation (Fig. 7A). Previously,  
460 Riebesell et al. (1991) suggested that less metabolically active sea ice algae were generally  
461 concentrated in aggregates, so we believe that the strong photooxidation state of the sediment  
462 trap material likely reflects a high contribution of aggregated senescent sea ice algae that  
463 sinks relatively slowly within the euphotic zone. Indeed, in dead cells or phytodetritus, there  
464 would be a shutdown of photosynthesis, such that an enhancement in the formation of excited  
465 chlorophyll (triplet) and  $^1\text{O}_2$  (exceeding the quenching capacity of the photoprotective system)  
466 would be expected (Nelson, 1993).

467 A further increase of the fluxes of  $\text{IP}_{25}$ , epi-brassicasterol, 24-methylenecholesterol,  
468 chl *a* and fatty acids occurred at 5 m towards the end of sampling between 17 June and 23  
469 June (Table 3, Figs. 5A, 6A and 8A and C). In these samples, chlorophyll (Fig. 5A), epi-  
470 brassicasterol (Fig. 8A) and 24-methylenecholesterol (Fig. 8C) were only weakly  
471 photodegraded, and significant photodegradation (ca. 50%) was only observed for palmitoleic

472 acid (Fig. 7A). These differences of photoreactivity are consistent with the involvement of  
473 steric hindrance during the attack of the sterol  $\Delta^5$  double bond by  $^1\text{O}_2$  (Beutner et al., 2000)  
474 and the contrasting sensitivity of these constituents towards photodegradation processes at  
475 low temperature and irradiance (Amiriaux et al., 2016). Indeed, during in vitro experiments  
476 carried out on senescent cells of the centric diatom *Chaetoceros neogracilis*, it was recently  
477 demonstrated that Type II photosensitized oxidation of palmitoleic acid was strongly  
478 enhanced by low temperatures and irradiances, while the opposite was true for the  
479 photodegradation of chl *a*. The strong increase of the (phytol + oxidation products)/IP<sub>25</sub> ratio  
480 during this later stage of sampling (values ranging from 2505–4353 g/g) suggests that the  
481 deposited material corresponded to a combination of partially degraded sea ice algae  
482 supplemented by pelagic algae in a healthy state. Similarly, Brown et al. (2016) reported that  
483 the proportion of ice-derived POC decreased from 28 to 13% at 5 m over the same period.  
484 However, since the sampling site remained ice-covered throughout the study (ice thickness >  
485 90 cm), we attribute this transition to an under-ice bloom (see Galindo et al., 2014; Mundy et  
486 al., 2014).

487 At 30 m, although the (phytol + oxidation products)/IP<sub>25</sub> ratios ( $292 \pm 138$  g/g) were  
488 still relatively close to those observed previously in the bottom ice samples (see above), the  
489 fluxes of IP<sub>25</sub> were higher than at 5 m (Table 3) indicating an even higher contribution of  
490 strongly aggregated sea ice algae to the material collected. However, in contrast to the 5 m  
491 samples, the C<sub>25:3</sub>(*E*)/IP<sub>25</sub> ratio in the 30 m sediment traps was consistently close to that  
492 measured in sea ice algae (Belt et al., 2013), while chlorophyll (Fig. 5D), epi-brassicasterol  
493 (Fig. 8B) and 24-methylcholesterol (Fig. 8D) were only weakly photodegraded, with only the  
494 very reactive palmitoleic acid exhibiting a degree of photodegradation similar to that seen in  
495 the samples collected at 5 m and towards the end of sampling (Fig. 7B). As such, we attribute  
496 the relative abiotic preservation of the material analyzed in the 30 m sediment traps to a high

497 contribution of highly aggregated senescent sea ice algae that settled rapidly out of the  
498 euphotic zone (Lalande et al., 2016).

499 The enhanced concentrations of chlorophyll and palmitoleic acids in the 30 m trap  
500 compared to the upper trap at 5 m probably results from their relatively higher abiotic  
501 preservation. In contrast, the highest amounts of saturated fatty acids (especially palmitic  
502 acid) at 30 m likely results from the presence of additional material derived from zooplankton  
503 at this depth. Consistent with this suggestion, we could also detect significant amounts of  
504  $C_{20:\Delta 11}$  and  $C_{22:\Delta 11}$  *n*-alkan-1-ols in some of the 30 m trap samples, which are typical of wax  
505 esters found in the large herbivorous copepods *Calanus hyperboreus* and *C. glacialis* that  
506 undergo diapause (Graeve et al., 1994).

507 Our combined lipid (parent and oxidation products) data can be represented by a 3-  
508 component conceptual scheme (Fig. 9) and described as follows: Ice algae released to the  
509 water column during ice melt either remain in suspension in the surface layer or are subject to  
510 rapid sinking to greater depths (Carey, 1987). The material remaining in suspension is  
511 composed mainly of unaggregated cells that are largely unstressed, despite the dramatic  
512 change of salinity that results during ice melt (Riebesell et al., 1991). Due to their healthy  
513 state, however, these cells may continue to grow in surface waters and are only weakly  
514 affected by Type II photosensitized oxidation processes. In contrast, those cells that are  
515 stressed as a result of the melt process occur in aggregates of varying sizes (Riebesell et al.,  
516 1991), the smallest being subject to a high degree of photooxidation, in part, due to their  
517 relatively slow sinking rate out of the euphotic zone. However, since unaggregated cells in the  
518 near surface waters do not appear to undergo the same degradation, our data indicate that the  
519 involvement of intense photooxidation requires the combination of four key parameters: an  
520 advanced senescent state of the cells, long residence times in the euphotic zone, low  
521 temperature, and low irradiance (Amiriaux et al., 2016). A significant part of this algal

522 material is also likely to undergo photodissolution before settling (Mayer et al. 2009). In  
523 contrast, the larger aggregates sink more rapidly out of the euphotic zone such that, despite  
524 their advanced senescent state, remain relatively preserved (unaffected by photodegradation)  
525 and likely contribute more strongly to the underlying sediments. As previously proposed by  
526 Riebesell et al. (1991), it seems that the process of aggregation acts as a mechanism for  
527 selection of cells less adapted to planktonic life.

528

## 529 **5. Conclusions**

530 By measuring various lipids and their characteristic oxidation products in suspended  
531 and sinking diatoms released from Arctic sea ice during a spring melt process, we have  
532 deduced that the nature and extent of degradation is quite variable, and is suggested to be  
533 attributable to the aggregation state of the cells and their physiological state. For example,  
534 suspended particles are mainly composed of growing cells with a high seeding potential for  
535 further growth, while metabolically less active cells are aggregated and concentrated in  
536 sinking particles. Due to their relatively slow sinking rate out of the euphotic zone and their  
537 advanced senescent state, the smallest aggregated sinking particles (collected at 5 m) are  
538 strongly photooxidized, while the larger aggregates (collected at 30 m) sink quickly out of the  
539 euphotic zone and remain relatively preserved. The very high photooxidation state of sinking  
540 particles collected at 5 m allowed us to confirm the strong efficiency of Type II  
541 photosensitized oxidation processes in senescent phytoplankton cells at low temperature and  
542 low irradiance previously observed in vitro.

543

## 544 **Acknowledgements**

545 This work was partially funded by the CNRS-INSU and the Aix-Marseille University.  
546 It was also funded by a Leverhulme Trust Research Project Grant, the University of

547 Plymouth, the Natural Sciences and Engineering Research Council of Canada (NSERC),  
548 Fonds de recherche du Québec—Nature et technologies (FRQNT), Canada Economic  
549 Development and the Polar Continental Shelf Program (PCSP) of Natural Resources Canada.  
550 The authors thank Christian Nozais for providing the sediment traps and Virginie Galindo,  
551 Mathew Gale, Marjolaine Blais and Joannie Charette for assistance in the field and/or the  
552 laboratory. This is a contribution to the research programs of ArcticNet, Québec-Océan,  
553 ISMER, Arctic Science Partnership (ASP) and the Canada Excellence Research Chair unit at  
554 the Centre for Earth Observation Science. We thank Dr. Sebastiaan Rampen and an  
555 anonymous reviewer for their useful and constructive comments.

556

557 *Associate Editor*—**Philip Meyers**

558

559 **References**

- 560 Amiraux, R., Jeanthon, C., Vaultier, F., Rontani, J.-F., 2016. Paradoxical effects of  
561 temperature and solar irradiance on the photodegradation state of killed phytoplankton.  
562 *Journal of Phycology* (in press).
- 563 Atlas, R.M., Bartha, R., 1992. Hydrocarbon biodegradation and oil spill bioremediation. In:  
564 Marshall, K.C. (Ed.), *Advances in Microbial Ecology*. Springer US, pp. 287–338.
- 565 Arrigo, K.R., Mock T., Lizotte M.P., Thomas D.N., Dieckmann G.S., 2010. Primary  
566 producers in sea ice. In: Thomas, D.N., Dieckmann, G.S. (Eds.), *Sea Ice*. 2nd ed.  
567 Wiley-Blackwell Publishing, Oxford, pp. 283–325.
- 568 Belt, S.T., Brown, T.A., Ringrose, A.E., Cabedo-Sanz, P., Mundy, C.J., Gosselin, M., Poulin,  
569 M., 2013. Quantitative measurement of the sea ice diatom biomarker IP<sub>25</sub> and sterols in  
570 Arctic sea ice and underlying sediments: Further considerations for palaeo sea ice  
571 reconstruction. *Organic Geochemistry* 62, 33–45.

- 572 Belt, S.T., Müller, J., 2013. The Arctic sea ice biomarker IP<sub>25</sub>: a review of current  
573 understanding, recommendations for future research and applications in palaeo sea ice  
574 reconstructions. *Quaternary Science Reviews* 79, 9–25.
- 575 Belt, S.T., Massé, G., Rowland, S.J., Poulin, M., Michel, C., LeBlanc, B., 2007. A novel  
576 chemical fossil of palaeo sea ice: IP<sub>25</sub>. *Organic Geochemistry* 38, 16–27.
- 577 Belt, S.T., Brown, T.A., Rodriguez, A.N., Sanz, P.C., Tonkin, A., Ingle, R., 2012. A  
578 reproducible method for the extraction, identification and quantification of the Arctic  
579 sea ice proxy IP<sub>25</sub> from marine sediments. *Analytical Methods* 4, 705.
- 580 Beutner, S., Bloedorn, B., Hoffmann, T., Martin, H.-D., 2000. Synthetic singlet oxygen  
581 quenchers. *Methods in Enzymology*, Elsevier, pp. 226–241.
- 582 Bowman, J.S., Rasmussen, S., Blom, N., Deming, J.W., Rysgaard, S., Sicheritz-Ponten, T.,  
583 2012. Microbial community structure of Arctic multiyear sea ice and surface seawater  
584 by 454 sequencing of the 16S RNA gene. *ISME Journal* 6, 11–20.
- 585 Brown, T.A., Belt, S.T., 2016. Novel tri- and tetra-unsaturated highly branched isoprenoid  
586 (HBI) alkenes from the marine diatom *Pleurosigma intermedium*. *Organic*  
587 *Geochemistry* 91, 120–122.
- 588 Brown, T.A., Belt, S.T., 2012a. Closely linked sea ice-pelagic coupling in the Amundsen Gulf  
589 revealed by the sea ice diatom biomarker IP<sub>25</sub>. *Journal of Plankton Research* 34, 647–  
590 654.
- 591 Brown, T.A., Belt, S.T., 2012b. Identification of the sea ice diatom biomarker IP<sub>25</sub> in Arctic  
592 benthic macrofauna: direct evidence for a sea ice diatom diet in Arctic heterotrophs.  
593 *Polar Biology* 35, 131–137.
- 594 Brown, T.A., Belt, S.T., Tatarek, A., Mundy, C.J., 2014. Source identification of the Arctic  
595 sea ice proxy IP<sub>25</sub>. *Nature Communications* 5. doi:10.1038/ncomms5197.



- 596 Brown, T.A., Belt, S.T., Gosselin, M., Levasseur, M., Poulin, M., Mundy, C.J., 2016.  
597 Quantitative estimates of sinking sea ice particulate organic carbon based on the  
598 biomarker IP<sub>25</sub>. Marine Ecology Progress Series (in press).
- 599 Brown, T.A., Belt, S.T., Philippe, B., Mundy, C.J., Massé, G., Poulin, M., Gosselin, M., 2011.  
600 Temporal and vertical variations of lipid biomarkers during a bottom ice diatom bloom  
601 in the Canadian Beaufort Sea: further evidence for the use of the IP<sub>25</sub> biomarker as a  
602 proxy for spring Arctic sea ice. Polar Biology 34, 1857–1868.
- 603 Carey, A.G., Boudrias, M.A., 1987. Feeding ecology of *Pseudalibrotus* (= *Onisimus*) *litoralis*  
604 Krøyer (Crustacea: Amphipoda) on the Beaufort Sea inner continental shelf. Polar  
605 Biology 8, 29–33.
- 606 Caron, D.A., Gast, R.J., 2010. Heterotrophic protists associated with sea ice. In: Thomas,  
607 D.N., Dieckmann, G.S. (Eds.), Sea Ice second ed., Wiley-Blackwell, Oxford, pp. 327–  
608 356.
- 609 Christodoulou, S., Marty, J.-C., Miquel, J.-C., Volkman, J.K., Rontani, J.-F., 2009. Use of  
610 lipids and their degradation products as biomarkers for carbon cycling in the  
611 northwestern Mediterranean Sea. Marine Chemistry 113, 25–40.
- 612 Christodoulou, S., Joux, F., Marty, J.-C., Sempéré, R., Rontani, J.-F., 2010. Comparative  
613 study of UV and visible light induced degradation of lipids in non-axenic senescent  
614 cells of *Emiliana huxleyi*. Marine Chemistry 119, 139–152.
- 615 Cuny, P., Rontani, J.-F., 1999. On the widespread occurrence of 3-methylidene-7,11,15-  
616 trimethylhexadecan-1,2-diol in the marine environment: a specific isoprenoid marker of  
617 chlorophyll photodegradation. Marine Chemistry 65, 155–165.
- 618 Cuny, P., Romano, J.-C., Beker, B., Rontani, J.-F., 1999. Comparison of the photodegradation  
619 rates of chlorophyll chlorin ring and phytol side chain in phytodetritus: is the phytyldiol

- 620 versus phytol ratio (CPPI) a new biogeochemical index? *Journal of Experimental*  
621 *Marine Biology and Ecology* 237, 271–290.
- 622 Curry, J.A., Schramm, J.L., Ebert, E.E., 1995. Sea ice-albedo climate feedback mechanism.  
623 *Journal of Climate* 8, 240–247.
- 624 Ehrenberg, B., Anderson, J.L., Foote, C.S., 1998. Kinetics and yield of singlet oxygen  
625 photosensitized by hypericin in organic and biological media. *Photochemistry and*  
626 *Photobiology* 68, 135–140.
- 627 Elliott, A., Mundy, C.J., Gosselin, M., Poulin, M., Campbell, K., Wang, F., 2015. Spring  
628 production of mycosporine-like amino acids and other UV-absorbing compounds in sea  
629 ice-associated algae communities in the Canadian Arctic. *Marine Ecology Progress*  
630 *Series* 541, 91–104.
- 631 Estapa, M.L., Mayer, L.M., 2010. Photooxidation of particulate organic matter,  
632 carbon/oxygen stoichiometry and related photoreactions. *Marine Chemistry* 122, 138–  
633 147.
- 634 Ewert, M., Deming, J.W., 2013. Sea ice microorganisms: Environmental constraints and  
635 extracellular responses. *Biology (Basel)* 2, 603–628.
- 636 Fahl, K., Kattner, G., 1993. Lipid content and fatty acid composition of algal communities in  
637 sea-ice and water from the Weddell Sea (Antarctica). *Polar Biology* 13, 405–409.
- 638 Ferrari, R., Jansen, M.F., Adkins, J.F., Burke, A., Stewart, A.L., Thompson, A.F., 2014.  
639 Antarctic sea ice control on ocean circulation in present and glacial climates.  
640 *Proceedings of the National Academy of Science* 111, 8753–8758.
- 641 Foote, C.S., 1976. Photosensitized oxidation and singlet oxygen: consequences in biological  
642 systems. In: Pryor, W.A. (Ed.), *Free Radicals in Biology*. Academic Press, New York,  
643 pp. 85–133.

- 644 Fortier, M., Fortier, L., Michel, C., Legendre, L., 2002. Climatic and biological forcing of the  
645 vertical flux of biogenic particles under seasonal Arctic sea ice. *Marine Ecology*  
646 *Progress Series* 225, 1–16.
- 647 Frankel, E.N., 1998. *Lipid Oxidation*. The Oily Press, Dundee.
- 648 Frankel, E.N., Neff, W.E., Bessler, T.R., 1979. Analysis of autoxidized fats by gas  
649 chromatography–mass spectrometry: V. Photosensitized oxidation. *Lipids* 14, 961–967.
- 650 Galindo, V., Levasseur, M., Scarratt, M., Mundy, C., Gosselin, M., Kiene, R., Gourdal, M.,  
651 Lizotte, M., 2015. Under-ice microbial dimethylsulfoniopropionate metabolism during  
652 the melt period in the Canadian Arctic Archipelago. *Marine Ecology Progress Series*  
653 524, 39–53.
- 654 Galindo, V., Levasseur, M., Mundy, C.J., Gosselin, M., Tremblay, J.-É., Scarratt, M., Gratton,  
655 Y., Papakiriakou, T., Poulin, M., Lizotte, M., 2014. Biological and physical processes  
656 influencing sea ice, under-ice algae, and dimethylsulfoniopropionate during spring in  
657 the Canadian Arctic Archipelago. *Journal of Geophysical Research: Oceans* 119, 3746–  
658 3766.
- 659 Girotti, A.W., 1998. Lipid hydroperoxide generation, turnover and effector action in  
660 biological systems. *Journal of Lipid Research* 39, 1529–1542.
- 661 Gosselin, M., Levasseur, M., Wheeler, P.A., Horner, R.A., Booth, B.C., 1997. New  
662 measurements of phytoplankton and ice algal production in the Arctic Ocean. *Deep Sea*  
663 *Research Part II: Topical Studies in Oceanography* 44, 1623–1644.
- 664 Graeve, M., Kattner, G., Hagen, W., 1994. Diet-induced changes in the fatty acid composition  
665 of Arctic herbivorous copepods, *Journal of Experimental Marine Biology and Ecology*  
666 182, 97–110.
- 667 Hargrave, B.T., Walsh, I.D., Murray, D.W., 2002. Seasonal and spatial patterns in mass and  
668 organic matter sedimentation in the North Water. *Deep Sea Research Part II: Topical*

- 669 Studies in Oceanography, The International North Water Polynya Study 49, 5227–  
670 5244.
- 671 Hartmann D.L., 1994. Global physical climatology. International Geophysics Series, Vol. 56.  
672 Academic Press, 412 pp.
- 673 Horner, R., Ackley, S., Dieckmann, G., Gulliksen, B., Hoshiai, T., Legendre, L., Melnikov, I.,  
674 Reeburgh, W., Spindler, M., Sullivan, C., 1992. Ecology of sea ice biota: 1. Habitat,  
675 terminology, and methodology. *Polar Biology* 12. doi:10.1007/BF00243113.
- 676 Knox, J.P., Dodge, A.D., 1985. Singlet oxygen and plants. *Phytochemistry* 24, 889–896.
- 677 Kulig, M.J., Smith, L.L., 1973. Sterol metabolism. XXV. Cholesterol oxidation by singlet  
678 molecular oxygen. *The Journal of Organic Chemistry* 38, 3639–3642.
- 679 Kessel, D., Smith, K., 1989. Photosensitization with derivatives of chlorophylls.  
680 *Photochemistry and Photobiology* 49, 157–160.
- 681 Lalande, C., Nöthig, E.-M., Bauerfeind, E., Hardge, K., Beszczynska-Möller, A., Fahl, K.,  
682 2016. Lateral supply and downward export of particulate matter from upper waters to  
683 the seafloor in the deep eastern Fram Strait. *Deep-Sea Research I* 114, 78–89.
- 684 Legendre, L., Ackley, S.F., Dieckmann, G.S., Gulliksen, B., Homer, R., Hoshiai, T.,  
685 Melnikov, I.A., Reeburgh, W.S., Spindler, M., Sullivan, C.W., 1992. Ecology of sea ice  
686 biota. 2. Global significance. *Polar Biology* 12, 429–444.
- 687 Leu, E., Wiktor, J.M., Søreide, J.E., Berge, J., Falk-Petersen, S., 2010. Fatty acid  
688 composition, element concentration and isotope ratios of sea ice algae sampled in  
689 Rijpfjorden, Svalbard, supplement to: Leu, Eva; Wiktor, Jozef M; Søreide, Janne E;  
690 Berge, J; Falk-Petersen, Stig (2010): Increased irradiance reduces food quality of sea  
691 ice algae. *Marine Ecology Progress Series* 411, 49–60.

- 692 Ligowski, R., Godlewski, M., Lukowski, A., 1992. Sea ice diatoms and ice edge planktonic  
693 diatoms at the northern limit of the Weddell Sea pack ice. Proceedings of the NIPR  
694 Symposium on Polar Biology 5, 9–20.
- 695 Marchand, D., Rontani, J.-F., 2001. Characterisation of photo-oxidation and autoxidation  
696 products of phytoplanktonic monounsaturated fatty acids in marine particulate matter  
697 and recent sediments. Organic Geochemistry 32, 287–304.
- 698 Mayer, L.M., Schick, L.L., Hardy, R., Estapa, M.L., 2009. Photodissolution and other  
699 photochemical changes upon irradiation of algal detritus. Limnology and  
700 Oceanography 54, 1688–1698.
- 701 Merzlyak, M.N., Hendry, G.A.F., 1994. Free radical metabolism, pigment degradation and  
702 lipid peroxidation in leaves during senescence. Proceedings of the Royal Society of  
703 Edinburgh B 102, 459–471.
- 704 Michel, C., Ingram, R.G., Harris, L.R., 2006. Variability in oceanographic and ecological  
705 processes in the Canadian Arctic Archipelago. Progress in Oceanography 71, 379–401.
- 706 Michel, C., Nielsen, T., Nozais, C., Gosselin, M., 2002. Significance of sedimentation and  
707 grazing by ice micro- and meiofauna for carbon cycling in annual sea ice (northern  
708 Baffin Bay). Aquatic Microbial Ecology 30, 57–68.
- 709 Mundy, C., Gosselin, M., Gratton, Y., Brown, K., Galindo, V., Campbell, K., Levasseur, M.,  
710 Barber, D., Papakyriakou, T., Bélanger, S., 2014. Role of environmental factors on  
711 phytoplankton bloom initiation under landfast sea ice in Resolute Passage, Canada.  
712 Marine Ecology Progress Series 497, 39–49.
- 713 Nelson, J.R., 1993. Rates and possible mechanism of light-dependent degradation of pigments  
714 in detritus derived from phytoplankton. Journal of Marine Research 51, 155–179.

- 715 Nozais, C., Gosselin, M., Michel, C., Tita, G., 2001. Abundance, biomass, composition and  
716 grazing impact of the sea-ice meiofauna in the North Water, northern Baffin Bay.  
717 *Marine Ecology Progress Series* 217, 235–250.
- 718 Parsons, T.R., Maita, Y., Lalli, C.M., 1984. *A Manual of Chemical and Biological Methods*  
719 *for Seawater Analysis*. Pergamon Press, Pons Point, NSW, Australia.
- 720 Porter, N.A., Caldwell, S.E., Mills, K.A., 1995. Mechanisms of free radical oxidation of  
721 unsaturated lipids. *Lipids* 30, 277–290.
- 722 Ralph, P.J., Ryan, K.G., Martin, A., Fenton, G., 2007. Melting out of sea ice causes greater  
723 photosynthetic stress in algae than freezing in. *Journal of Phycology* 43, 948–956.
- 724 Rampen, S.W., Abbas, B.A., Schouten, S., Sinninghe Damsté, J.S., 2010. A comprehensive  
725 study of sterols in marine diatoms (Bacillariophyta): implications for their use as  
726 tracers for diatom productivity. *Limnology and Oceanography* 55, 91–105
- 727 Renaud, P.E., Morata, N., Ambrose Jr., W.G., Bowie, J.J., Chiuchiolo, A., 2007. Carbon  
728 cycling by seafloor communities on the eastern Beaufort Sea shelf. *Journal of*  
729 *Experimental Marine Biology and Ecology* 349, 248–260.
- 730 Riebesell, U., Schloss, I., Smetacek, V., 1991. Aggregation of algae released from melting sea  
731 ice -implications for seeding and sedimentation. *Polar Biology* 11, 239–248.
- 732 Rontani, J.-F., 2008. Photooxidative and autoxidative degradation of lipid components during  
733 the senescence of phototrophic organisms. In: Matsumoto, T. (Ed.), *Phytochemistry*  
734 *Research Progress*. Nova Science Publishers, pp. 115–154.
- 735 Rontani, J.-F., 2012. Photo- and free radical-mediated oxidation of lipid components during  
736 the senescence of phototrophic organisms. In: Nagata, T. (Ed.), *Senescence*. Intech,  
737 Rijeka, pp. 3–31.
- 738 Rontani, J.-F., Marchand, D., 2000. Photoproducts of phytoplanktonic sterols: a potential  
739 source of hydroperoxides in marine sediments? *Organic Geochemistry* 31, 169–180.

- 740 Rontani, J.-F., Aubert, C., 2005. Characterization of isomeric allylic diols resulting from  
741 chlorophyll phytyl side-chain photo- and autoxidation by electron ionization gas  
742 chromatography/mass spectrometry. *Rapid Communications in Mass Spectrometry* 19,  
743 637–646.
- 744 Rontani, J.-F., Raphel, D., Cuny, P., 1996. Early diagenesis of the intact and photooxidized  
745 chlorophyll phytyl chain in a recent temperate sediment. *Organic Geochemistry* 24,  
746 825–832.
- 747 Rontani, J.-F., Cuny, P., Grossi, V., 1998. Identification of a “pool” of lipid photoproducts in  
748 senescent phytoplanktonic cells. *Organic Geochemistry* 29, 1215–1225.
- 749 Rontani, J.-F., Zabeti, N., Wakeham, S.G., 2009. The fate of marine lipids: Biotic vs. abiotic  
750 degradation of particulate sterols and alkenones in the Northwestern Mediterranean  
751 Sea. *Marine Chemistry* 113, 9–18.
- 752 Rontani, J.-F., Grossi, V., Faure, R., Aubert, C., 1994. “Bound” 3-methylidene-7,11,15-  
753 trimethylhexadecan-1,2-diol: a new isoprenoid marker for the photodegradation of  
754 chlorophyll-a in seawater. *Organic Geochemistry* 21, 135–142.
- 755 Rontani, J.F., Rabourdin, A., Marchand, D., Aubert, C., 2003. Photochemical oxidation and  
756 autoxidation of chlorophyll phytyl side chain in senescent phytoplanktonic cells:  
757 Potential sources of several acyclic isoprenoid compounds in the marine environment.  
758 *Lipids* 38, 241–254.
- 759 Rontani, J.-F., Belt, S.T., Vaultier, F., Brown, T.A., 2011. Visible light induced photo-  
760 oxidation of highly branched isoprenoid (HBI) alkenes: Significant dependence on the  
761 number and nature of double bonds. *Organic Geochemistry* 42, 812–822.
- 762 Rontani, J.-F., Belt, S.T., Brown, T.A., Vaultier, F., Mundy, C.J., 2014. Sequential photo- and  
763 autoxidation of diatom lipids in Arctic sea ice. *Organic Geochemistry* 77, 59–71.

- 764 Rontani, J.-F., Rabourdin, A., Pinot, F., Kandel, S., Aubert, C., 2005. Visible light-induced  
765 oxidation of unsaturated components of cutins: a significant process during the  
766 senescence of higher plants. *Phytochemistry* 66, 313–321.
- 767 Rontani, J.-F., Charriere, B., Forest, A., Heussner, S., Vaultier, F., Petit, M., Delsaut, N.,  
768 Fortier, L., Sempéré, R., 2012. Intense photooxidative degradation of planktonic and  
769 bacterial lipids in sinking particles collected with sediment traps across the Canadian  
770 Beaufort Shelf (Arctic Ocean). *Biogeosciences* 9, 4787–4802.
- 771 Róžańska, M., Gosselin, M., Poulin, M., Wiktor, J., Michel, C., 2009. Influence of  
772 environmental factors on the development of bottom ice protist communities during the  
773 winter–spring transition. *Marine Ecology Progress Series* 386, 43–59.
- 774 Smith, L.L., 1981. *Cholesterol Autoxidation*. Springer Science & Business Media.
- 775 Suh, H.-J., Lee, H.-W., Jung, J., 2003. Mycosporine glycine protects biological systems  
776 against photodynamic damage by quenching singlet oxygen with a high efficiency.  
777 *Photochemistry and Photobiology* 78, 109–113.
- 778 Suwa, K., Kimura, T., Schaap, A.P., 1977. Reactivity of singlet molecular oxygen with  
779 cholesterol in a phospholipidic membrane matrix: a model for oxidative damage of  
780 membranes. *Biochemistry and Biophysical Research Communications* 75, 785–792.
- 781 Tedesco, M., Fettweis, X., 2012. 21st century projections of surface mass balance changes for  
782 major drainage systems of the Greenland ice sheet. *Environmental Research Letters* 7,  
783 045405. doi:10.1088/1748-9326/7/4/045405
- 784 Vancoppenolle, M., Meiners, K.M., Michel, C., Bopp, L., Brabant, F., Carnat, G., Delille, B.,  
785 Lannuzel, D., Madec, G., Moreau, S., Tison, J.-L., van der Merwe, P., 2013. Role of  
786 sea ice in global biogeochemical cycles: emerging views and challenges. *Quaternary*  
787 *Science Reviews*, 79, 207–230.



- 788 Volkman, J.K., 1986. A review of sterol markers for marine and terrigenous organic matter.  
789           Organic Geochemistry 9, 83–99.
- 790 Volkman, J.K., 2003. Sterols in microorganisms. Applied Microbiology and Biotechnology  
791           60, 495–506.
- 792 Volkman, J.K., 2005. Sterols and other triterpenoids: source specificity and evolution of  
793           biosynthetic pathways. Organic Geochemistry 36, 139–159.
- 794 Zafiriou, O.C., Jousset-Dubien, J., Zepp, R.G., Zika, R.G., 1984. Photochemistry of natural  
795           waters. Environmental Science and Technology 18, 358–371.
- 796

797 FIGURE CAPTIONS

798

799 **Fig. 1.** Structures and potential applications of the different lipid tracers of degradation

800 processes used in the present work. <sup>1</sup>Hydroperoxides were quantified after NaBH<sub>4</sub>-reduction  
801 to the corresponding alcohols.

802

803 **Fig. 2.** Estimates of chlorophyll *a* photooxidation in suspended particles collected at 2 m (A),  
804 5 m (B) and 10 m (C).

805

806 **Fig. 3.** Fatty acid concentrations in suspended particles collected at 2 m (A), 5 m (B) and 10  
807 m (C).

808

809 **Fig. 4.** Photo- and autoxidation percentages in suspended particles collected at 2 m (A), 5 m  
810 (B) and 10 m (C).

811

812 **Fig. 5.** Estimates of fluxes of chlorophyll *a* and chlorophyll photooxidation in sediment traps  
813 at 5 m (A and B) and at 30 m (C and D).

814

815 **Fig. 6.** Fluxes of fatty acids in sediment traps at 5 m (A) and 30 m (B).

816

817 **Fig. 7.** Photo- and autoxidation percentages of palmitoleic acid in sediment traps at 5 m (A)  
818 and 30 m (B).

819

820 **Fig. 8.** Fluxes of epi-brassicasterol and 24-methylenecholesterol and their photooxidation  
821 products in sediment traps at 5 m (A and C) and at 30 m (B and D).

822

823 **Fig. 9.** Three-component conceptual scheme summarizing the behavior of algae released to

824 the water column during ice melt in Resolute Bay (Canadian Arctic).

825

ACCEPTED MANUSCRIPT

Disclaimer: This is a pre-publication version. Readers are recommended to consult the full published version for accuracy and citation.

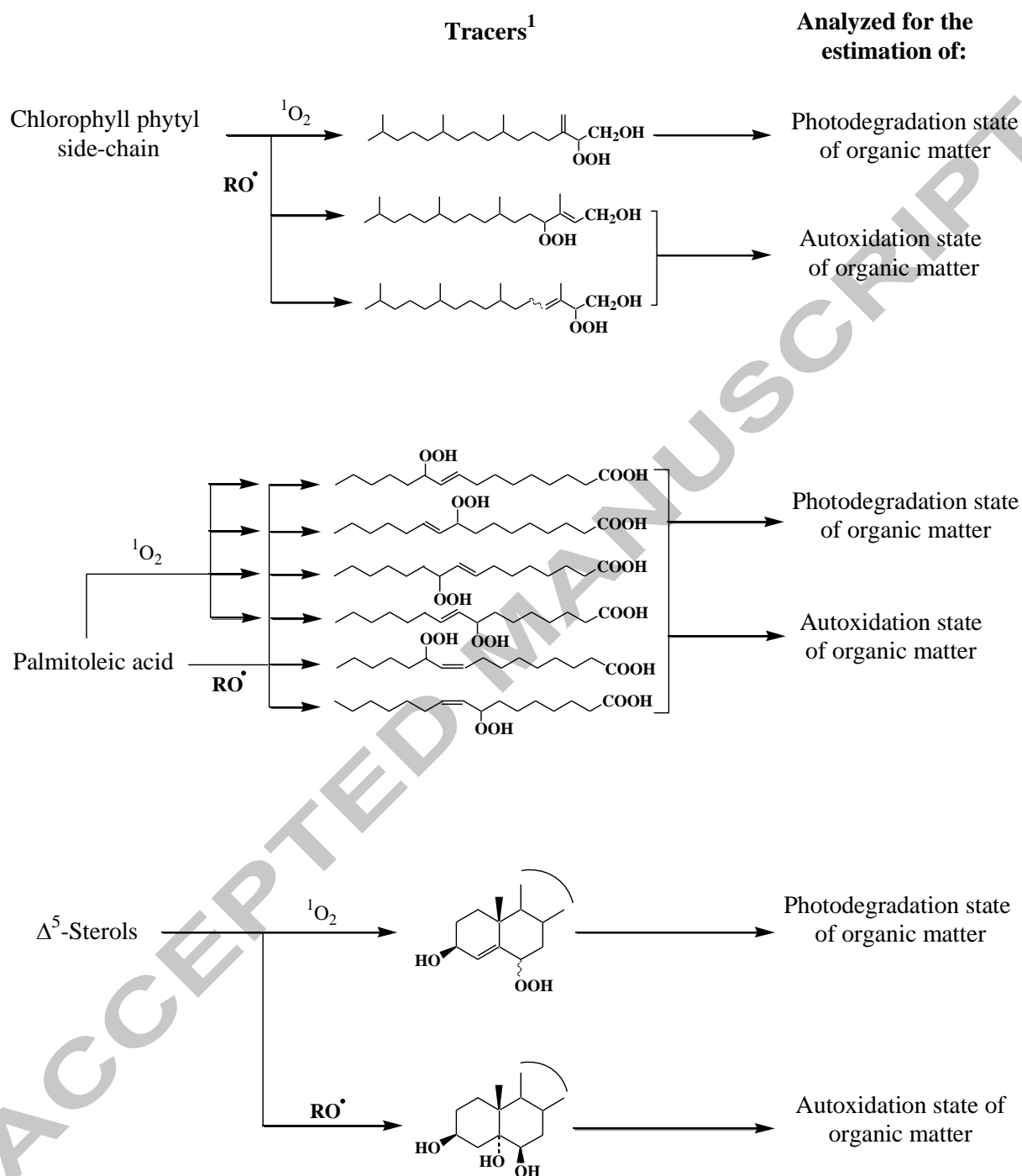
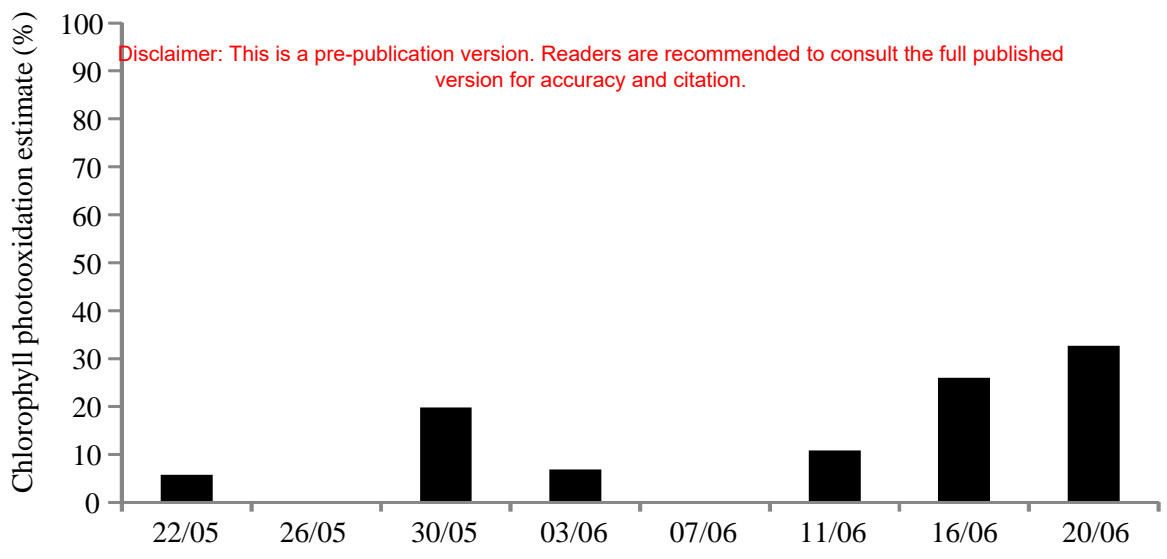
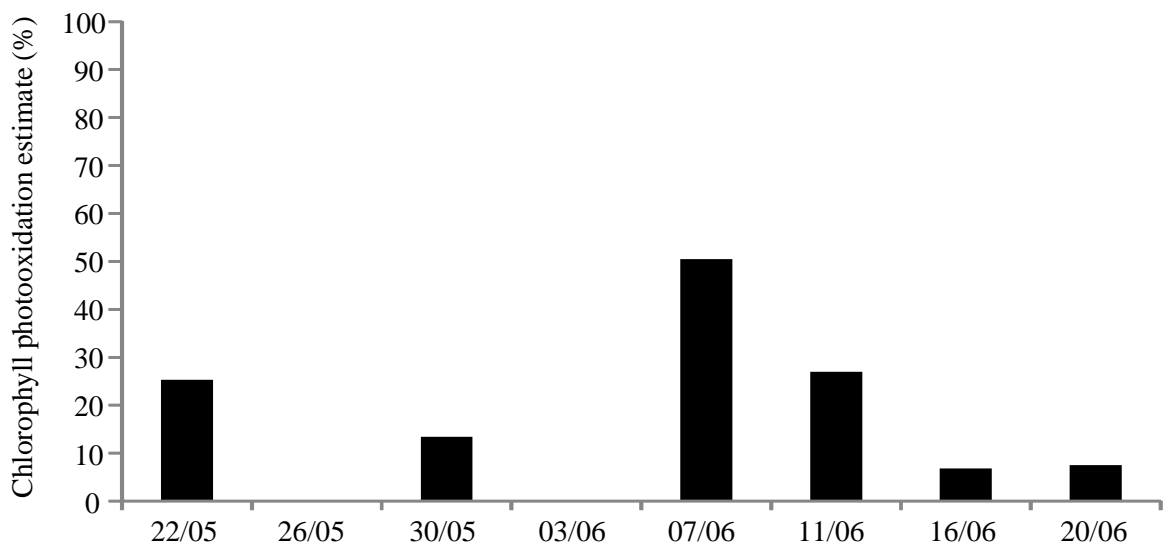


**Figure 2**

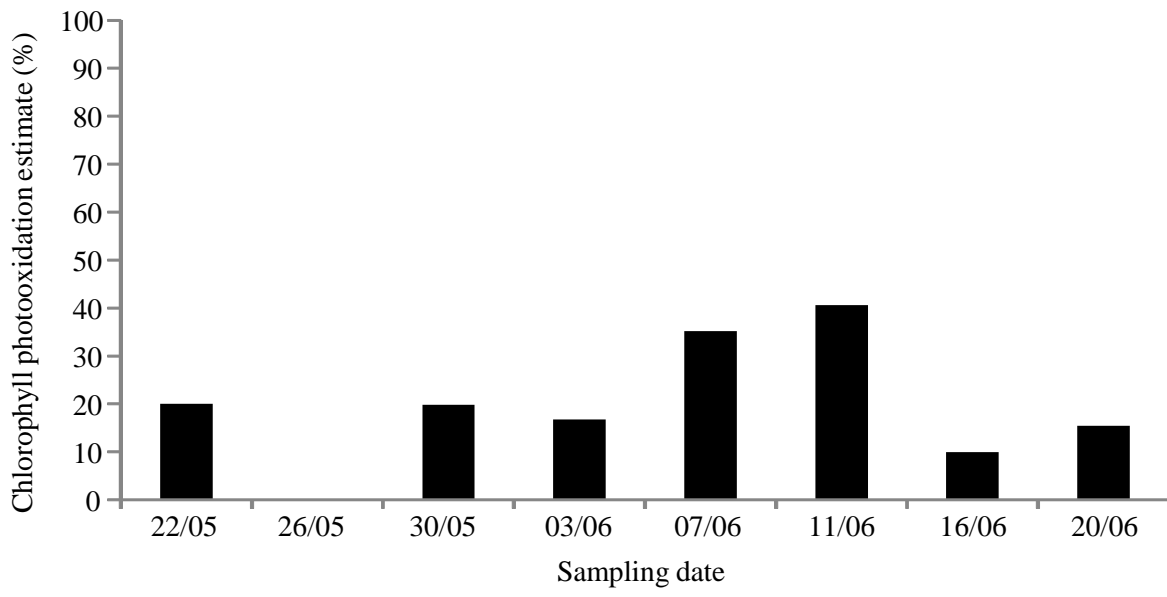
**A**

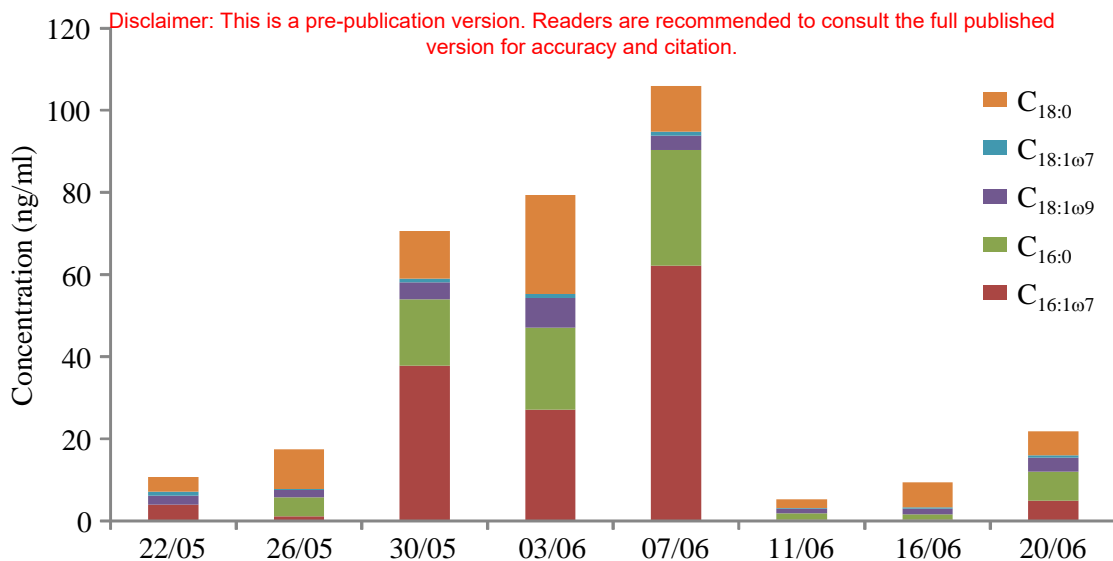
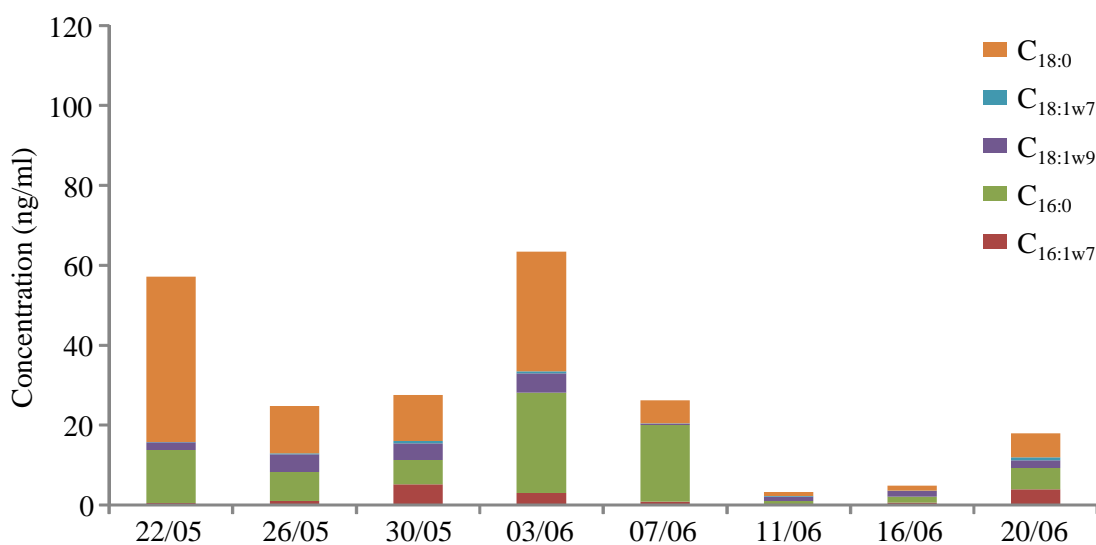
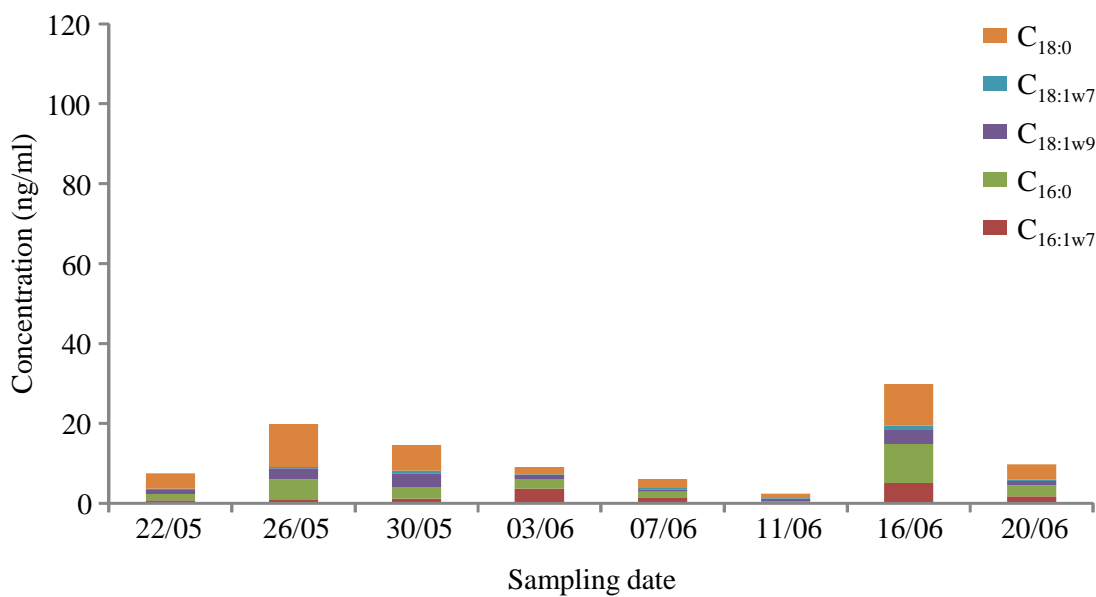


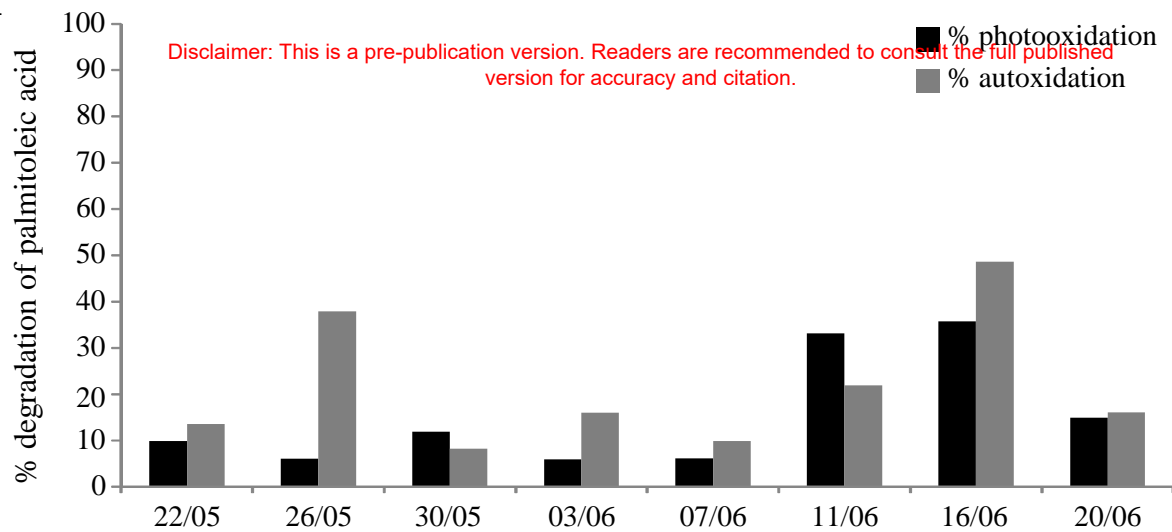
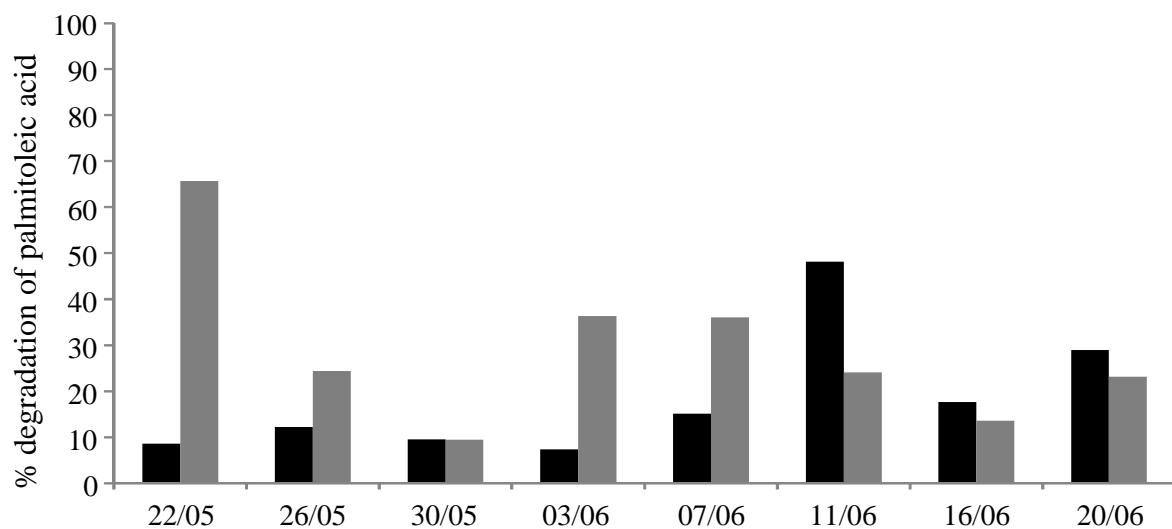
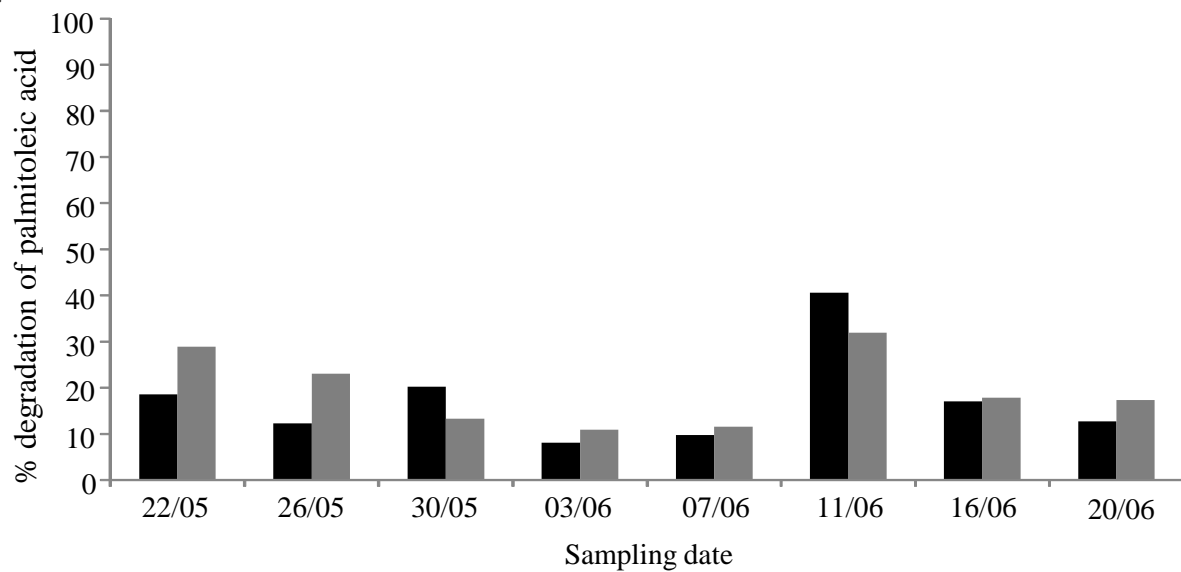
**B**



**C**

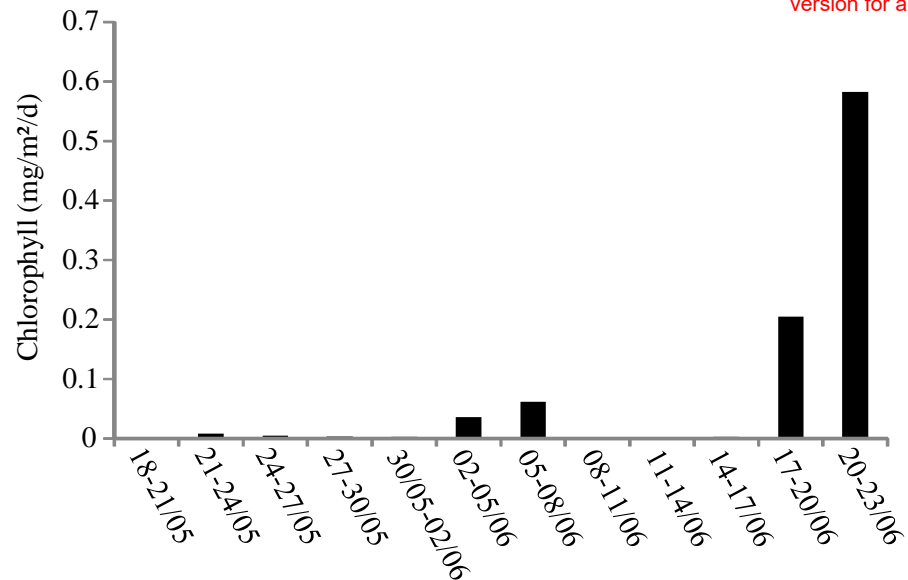
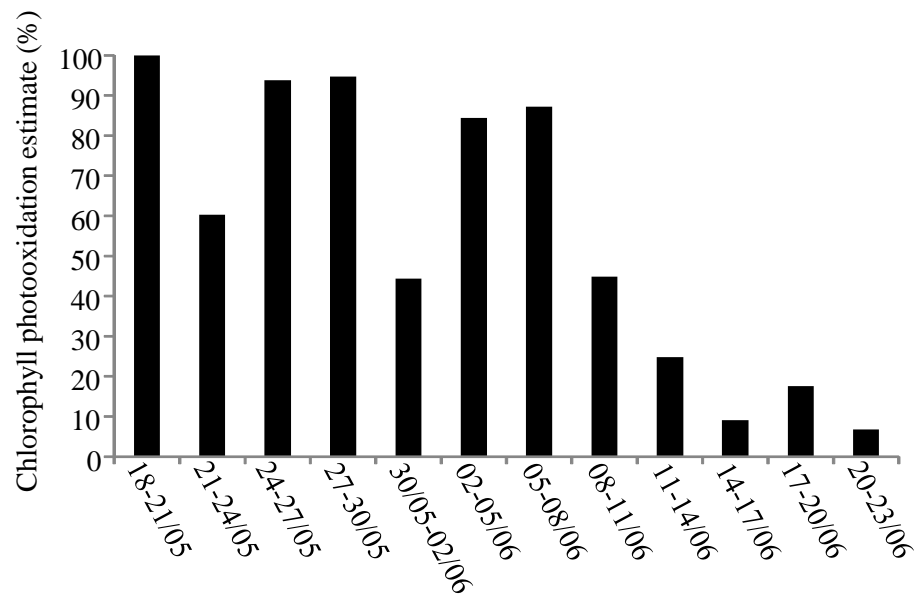
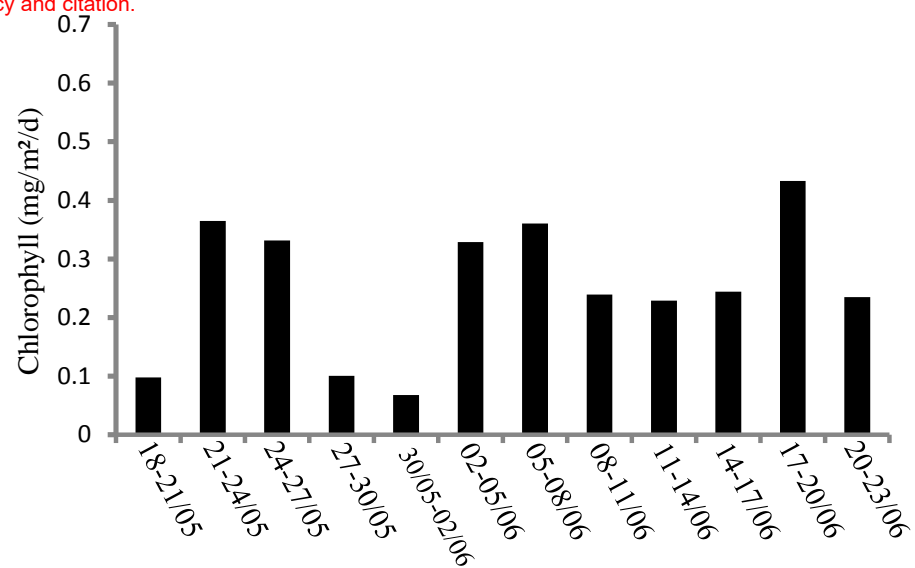
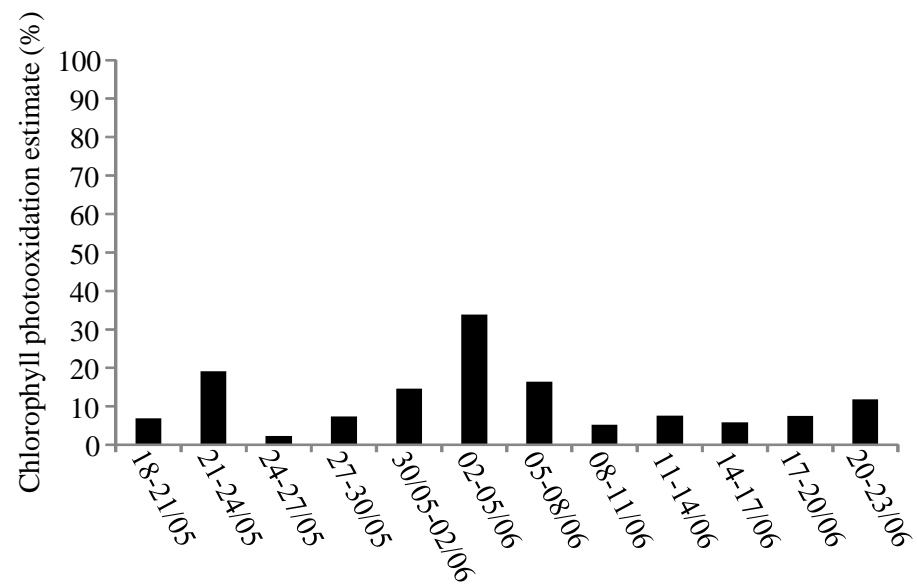


**Figure 3****A****B****C**

**Figure 4****A****B****C**

**Figure 5****A**

Disclaimer: This is a pre-publication version. Readers are recommended to consult the full published version for accuracy and citation.

**B****C****D**



**Figure 6**

Disclaimer: This is a pre-publication version. Readers are recommended to consult the full published version for accuracy and citation.

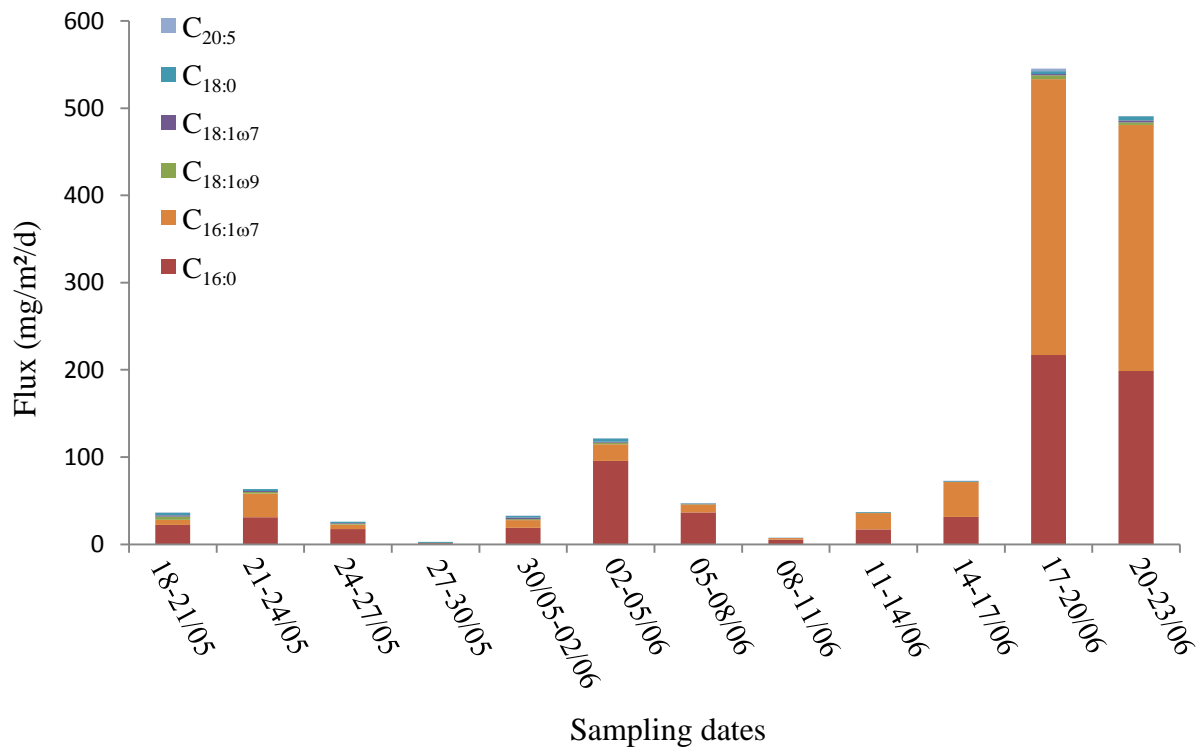
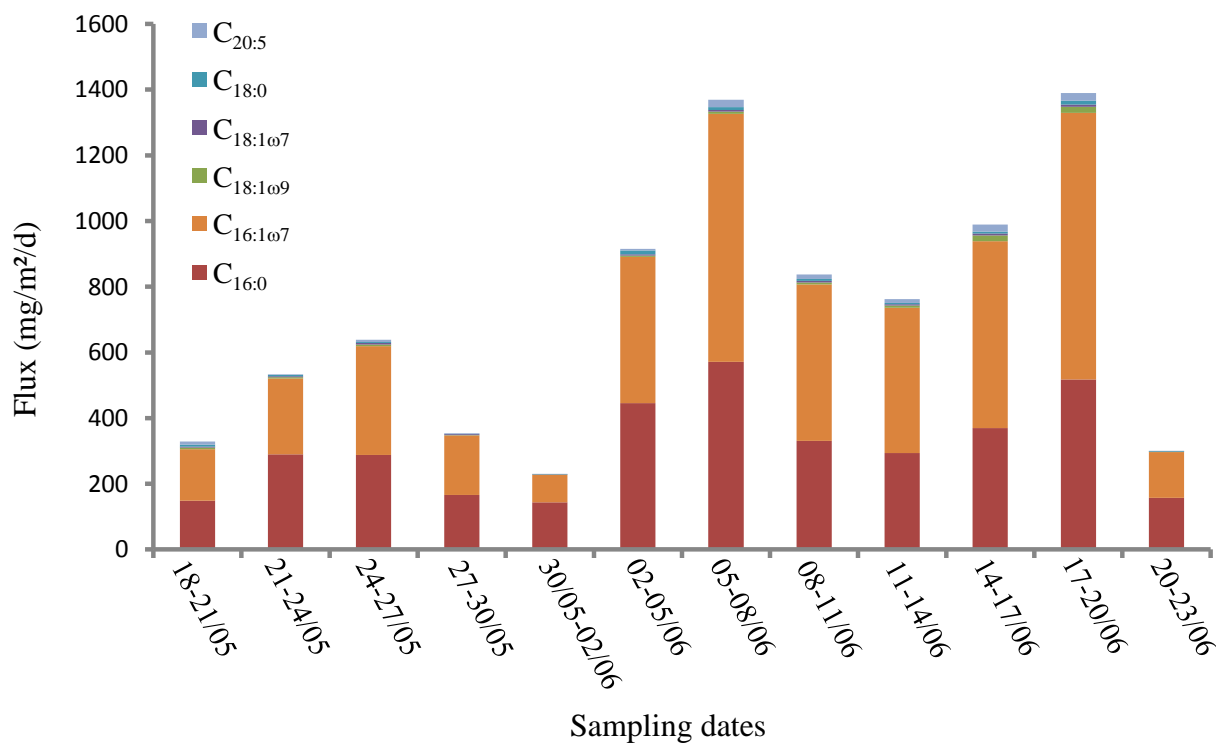
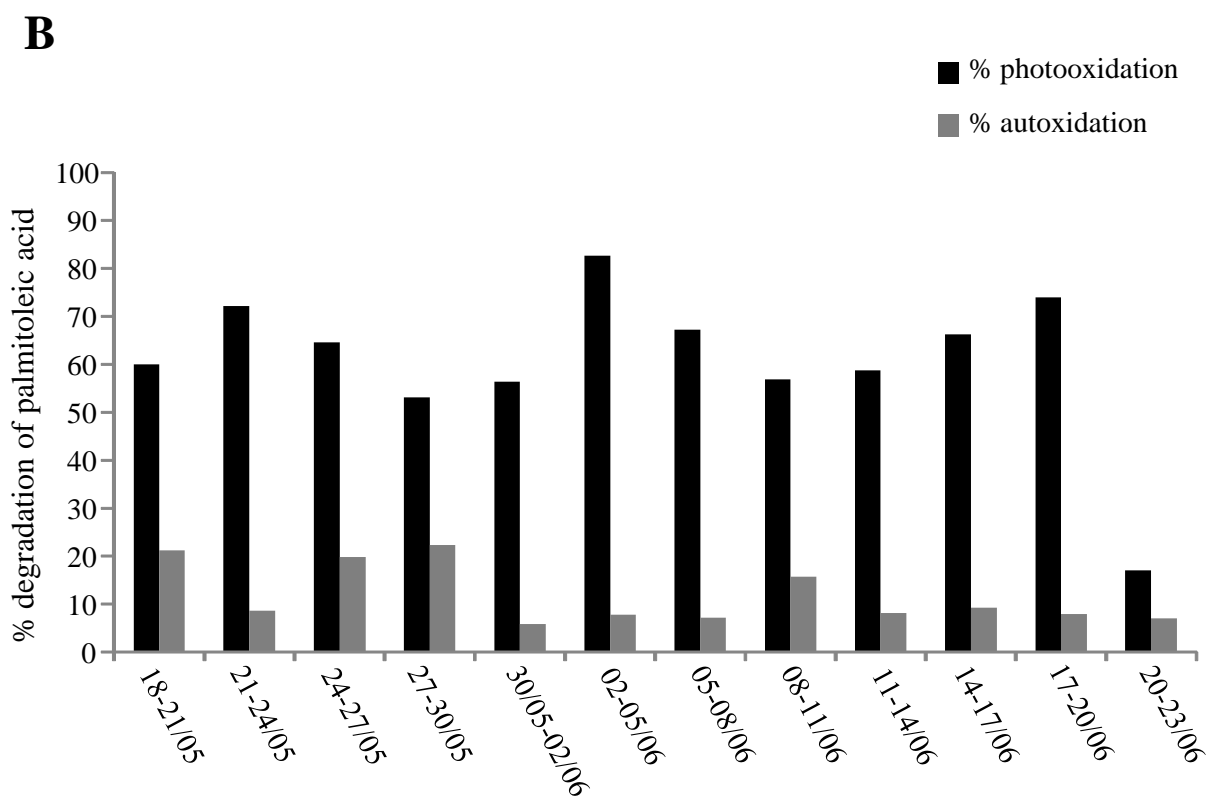
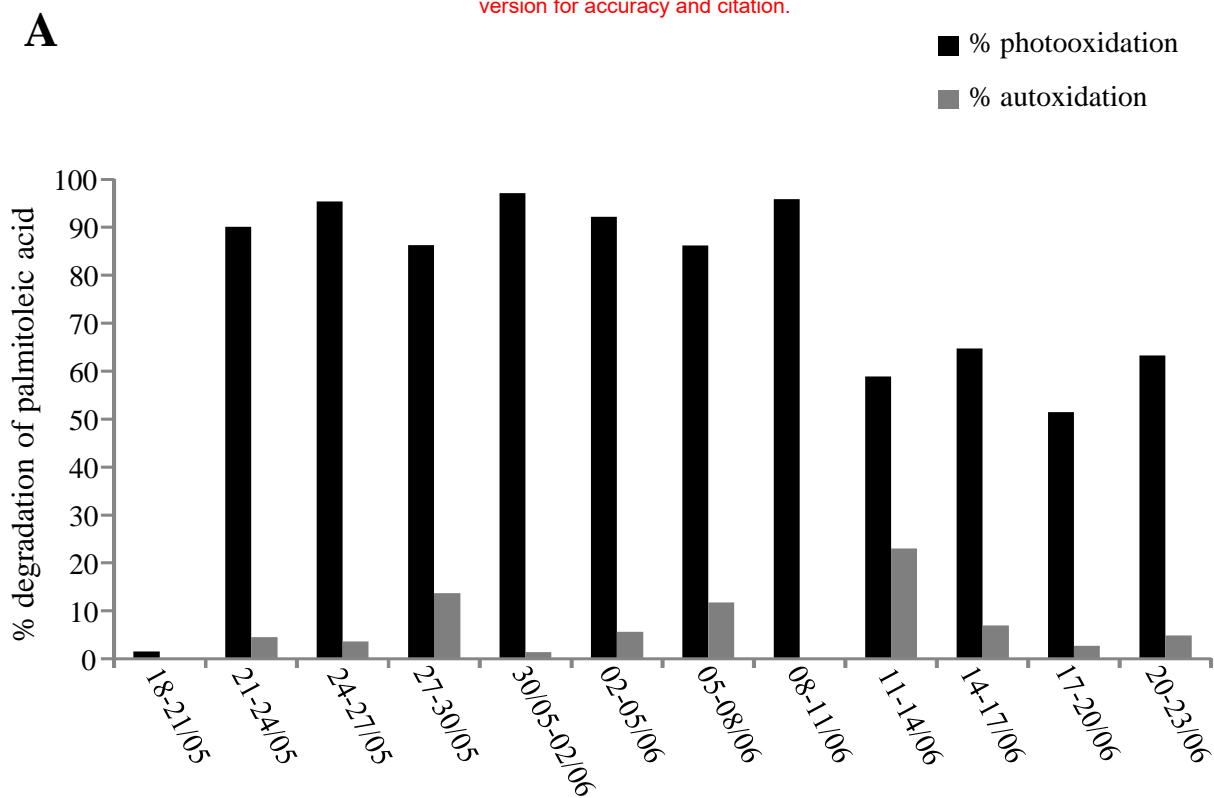
**A****B**

Figure 7

Disclaimer: This is a pre-publication version. Readers are recommended to consult the full published version for accuracy and citation.

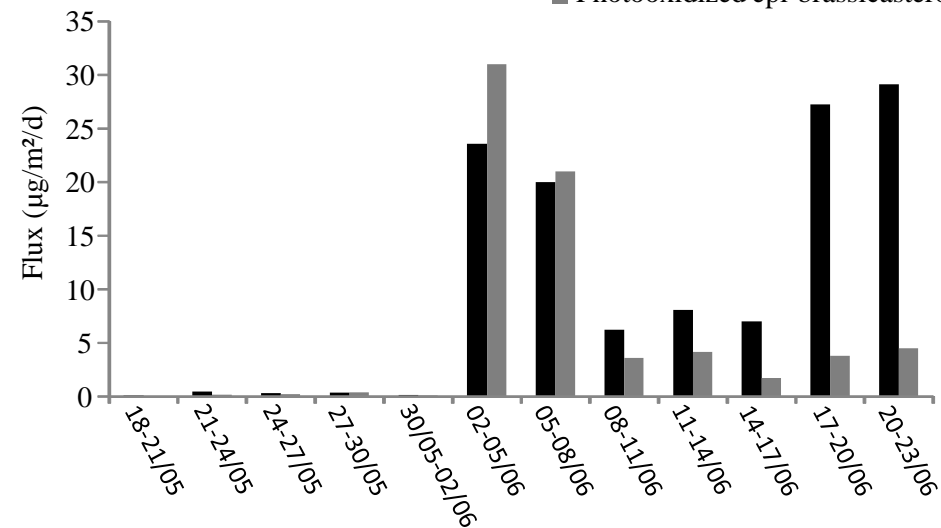


**Figure 8****A**

Disclaimer: This is a pre-publication version. Readers are recommended to consult the full published version for accuracy and citation.

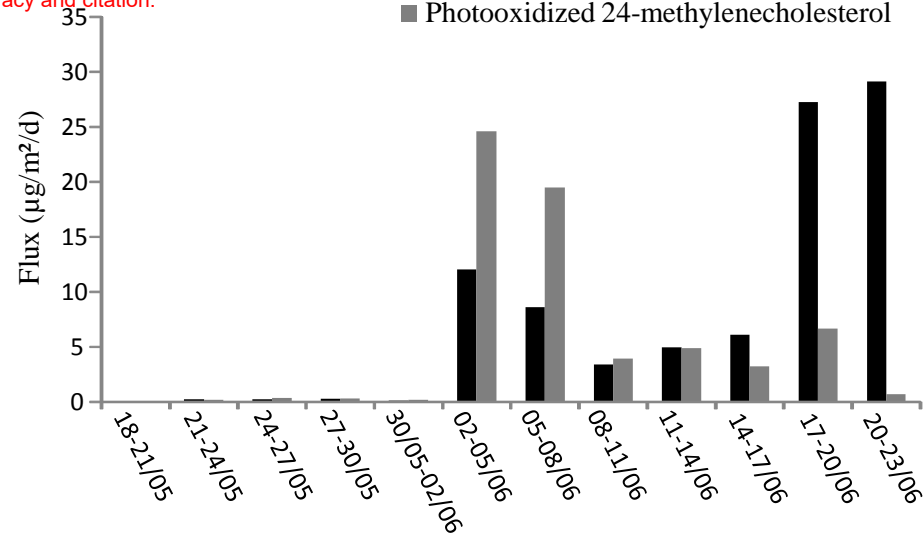
■ Epi-brassicasterol

■ Photooxidized epi-brassicasterol

**C**

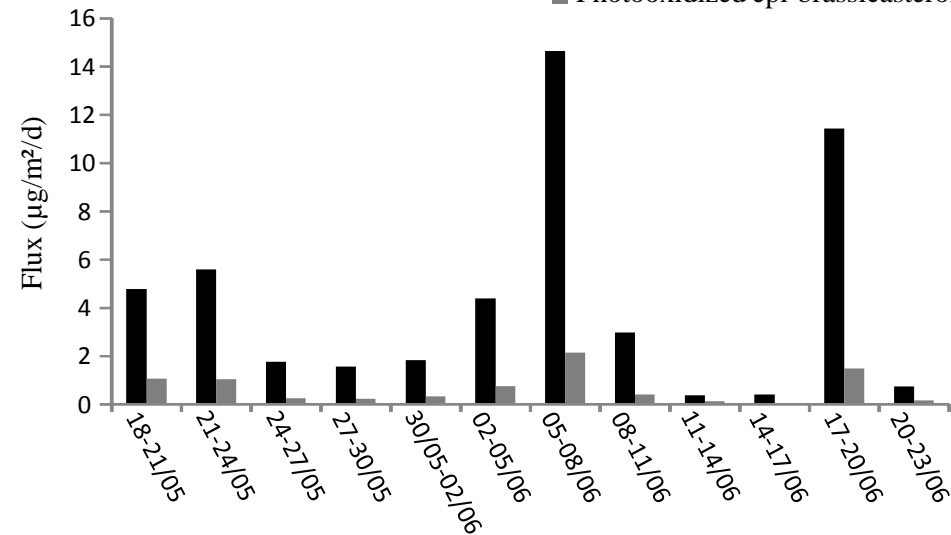
■ 24-Methylenecholesterol

■ Photooxidized 24-methylenecholesterol

**B**

■ Epi-brassicasterol

■ Photooxidized epi-brassicasterol

**D**

■ 24-Methylenecholesterol

■ Photooxidized 24-methylenecholesterol

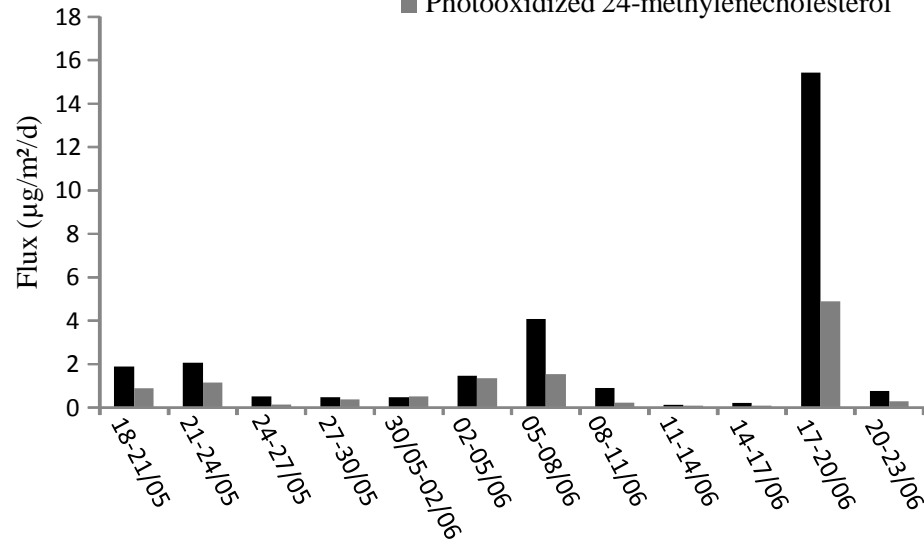
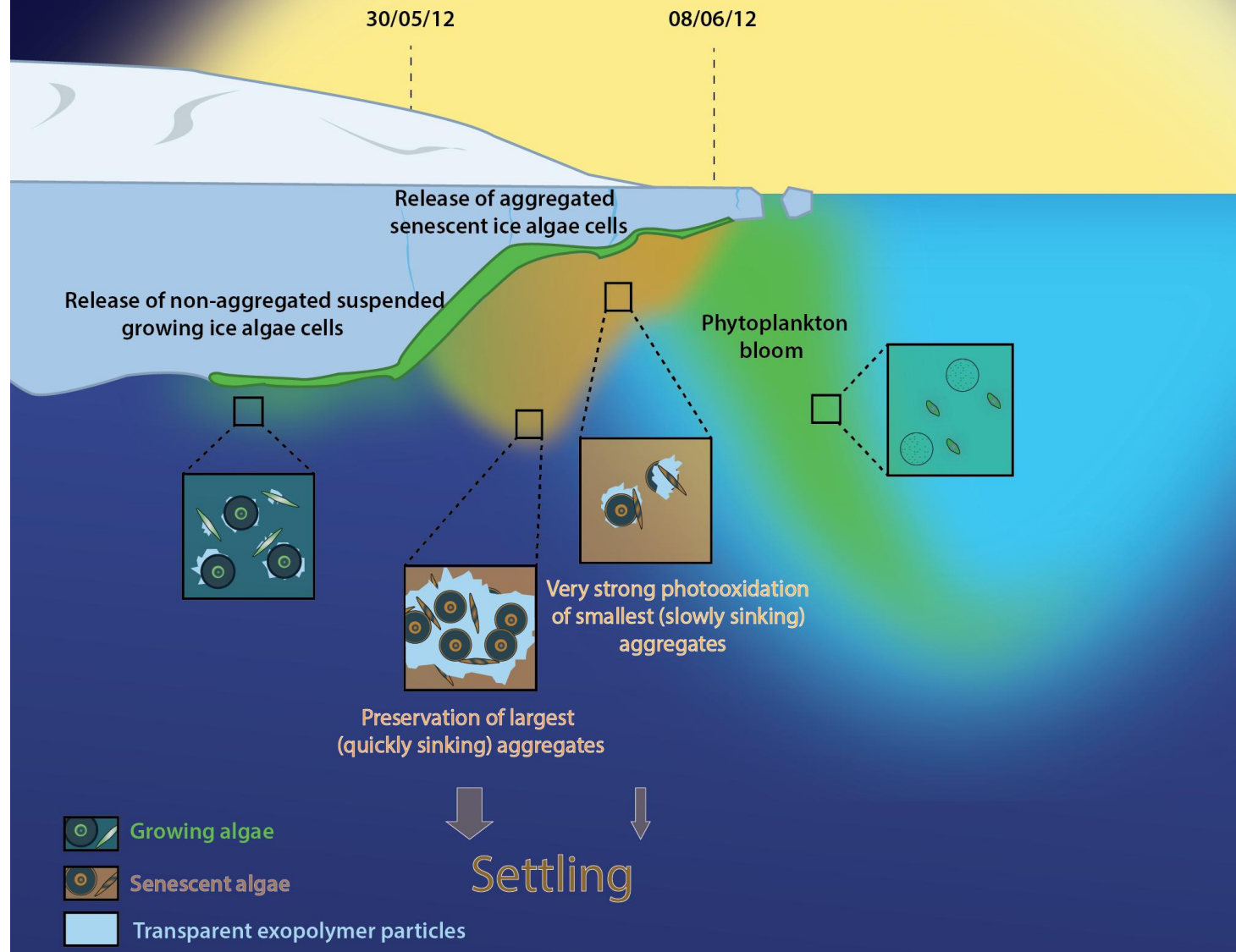


Figure 9

Disclaimer: This is a pre-publication version. Readers are recommended to consult the full published version for accuracy and citation.



826

827

828 **Table 1**829 Concentrations (ng/ml) of chlorophyll-*a* and  $\Delta^5$ -sterols in SPM samples.

830

Sampling dates	22/05/20 12			26/05/20 12			30/05/20 12			03/06/20 12			07/06/20 12			11/06/20 12			16/06/20 12			20/06/20 12		
Depth (m)	2	5	1	2	5	1	2	5	1	2	5	1	2	5	1	2	5	1	2	5	1	2	5	1
Chlorophyll <i>a</i>	0	0	0	0	0	0	0	0	0	1	0	0	1	0	0	1	0	0	0	0	0	0	0	0
	3	3	3	3	1	3	6	1	2	5	4	2	1	4	4	6	7	3	2	3	1	4	3	4
	6	5	0	4	5	9	5	7	2	4	2	6	7	3	1	5	0	8	2	1	8	8	7	4
Epi-brassica sterol	0	0	0	0	0	0	0	0	0	0	0	0	0	0	0	0	0	0	0	0	0	0	0	0
	0	0	0	0	0	0	0	0	0	1	0	0	2	nd	0	0	0	0	0	0	1	0	0	0
	6	2	4	1	3	2	8	3	1	2	3	8	4	*	3	5	4	5	9	1	0	4	7	3
24-Methylncholesterol	0	0	0	nd	0	0	0	0	0	0	0	0	0	nd	0	0	0	0	0	0	nd	0	0	0
	0	0	0	0	0	0	0	0	0	0	0	0	1	0	0	0	0	0	0	0	0	0	0	0
	3	1	2	1	1	4	2	1	4	1	3	5	2	2	3	2	3	4	4	5	1	2	1	1

831 \* nd: not detected

832

833 **Table 2**

834 Concentrations of 2,6,10,14-tetramethyl-7-(3-methylpent-4-enyl)-pentadecane (IP<sub>25</sub>) and  
 835 2,6,10,14-tetramethyl-7-(3-methylpenta-1,4-dienyl)-pentadeca-7(20*E*),9*E*-diene (C<sub>25:3</sub>(*E*)) in  
 836 the different SPM samples analyzed.

Sampling date	Depth (m)	IP <sub>25</sub> (ng/ml)	C <sub>25:3</sub> ( <i>E</i> ) ng/ml	C <sub>25:3</sub> ( <i>E</i> )/IP <sub>25</sub>
22/05/2012	2	14.7	3.27	0.222
	5	7.4	2.67	0.361
	10	8.6	2.70	0.313
26/05/2012	2	13.0	2.59	0.200
	5	11.5	3.60	0.313
	10	12.7	3.37	0.265
30/05/2012	2	64.4	10.3	0.153
	5	2.1	0.84	0.400
	10	7.7	1.79	0.232
03/06/2012	2	19.7	5.94	0.301
	5	16.8	3.01	0.179
	10	15.5	2.69	0.173
07/06/2012	2	41.6	na <sup>\$</sup>	
	5	17.6	na	
	10	17.5	na	
11/06/2012	2	7.0	nd*	0
	5	9.5	nd	0
	10	12.3	nd	0
16/06/2012	2	9.3	0.47	0.051
	5	14.6	nd	0
	10	14.6	nd	0
20/06/2012	2	30.3	nd	0
	5	15.7	nd	0
	10	15.6	nd	0
23/06/2012	2	12.6	nd	0
	5	13.1	nd	0
	10	14.1	nd	0

837 \* nd: not detected (S/N > 3)

838 <sup>\$</sup> na : not analyzed (contamination)

839

840 **Table 3**

841 Fluxes of 2,6,10,14-tetramethyl-7-(3-methylpent-4-enyl)-pentadecane (IP<sub>25</sub>) and 2,6,10,14-  
 842 tetramethyl-7-(3-methylpenta-1,4-dienyl)-pentadeca-7(20*E*),9*E*-diene (C<sub>25:3</sub>(*E*)) in the  
 843 different trap samples analyzed.

Sampling dates	Depth (m)	IP <sub>25</sub> (ng/m <sup>2</sup> /d)	C <sub>25:3</sub> ( <i>E</i> ) (ng/m <sup>2</sup> /d)	C <sub>25:3</sub> ( <i>E</i> )/IP <sub>25</sub>
18-21/05/2012	5	1.10	nd*	0
	30	na <sup>§</sup>	na	
21-24/05/2012	5	2.25	nd	0
	30	na	na	
24-27/05/2012	5	1.67	nd	0
	30	5.51	1.03	0.187
27-30/05/2012	5	1.81	nd	0
	30	3.79	0.13	0.033
30/05-02/06/2012	5	1.30	nd	0
	30	2.68	0.28	0.103
02-05/06/2012	5	3.08	0.04	0.014
	30	6.77	1.02	0.151
05-08/06/2012	5	3.96	0.09	0.023
	30	7.59	1.40	0.184
08-11/06/2012	5	0.60	nd	0
	30	10.19	1.22	0.120
11-14/06/2012	5	1.43	nd	0
	30	5.37	0.96	0.180
14-17/06/2012	5	1.16	nd	0
	30	8.27	1.67	0.202
17-20/06/2012	5	2.44	0.16	0.065
	30	3.42	0.49	0.144
20-23/06/2012	5	4.38	0.54	0.124
	30	1.59	0.18	0.115

844 \* nd: not detected (S/N > 3)

845 § na : not analyzed.

846

- 847 Lipid degradation products were analyzed in particles collected in the Arctic
- 848 Suspended particles appeared to be composed of unaggregated living cells
- 849 Photooxidation processes act strongly in slowly sinking aggregated cells
- 850 The larger aggregates sink quickly and escape photooxidation
- 851 Aggregation plays a key role in the degradation of sea ice algae
- 852

ACCEPTED MANUSCRIPT